NASA Contractor Report 178249

TURBULENCE CONTROL OF AN AIRBORNE LASER PLATFORM

Mohamed Gad-el-Hak

FLOW INDUSTRIES, INC.
Flow Research Company
Kent, Washington

Contract NAS1-18213
March 1987

National Aeronautics and
Space Administration

Langley Research Center
Hampton, Virginia 23665

NATIONAL AERONAUTICS AND SPACE ADMINISTRATION

PHASE I SBIR - FINAL TECHNICAL REPORT

PROJECT SUMMARY

PROJECT TITLE	:	Turbulence Control on An Airborne Laser Platform
CONTRACT NUMBER	:	NAS1-18213
ISSUED BY	:	NASA-Langley Research Center
TECHNICAL MONITOR	:	John C. Lin
CONTRACTOR	:	Flow Industries, Inc.
PRINCIPAL INVESTIGATOR	:	Mohamed Gad-el-Hak
DURATION	:	1 January 1986 - 30 June 1986

An active flow control device to generate large-scale, periodic structures in a turbulent shear flow is developed. Together with adaptive optics, the device may be used on airborne laser platforms to reduce or eliminate optical distortion caused by the turbulence in the aircraft's boundary layer. A cyclic jet issuing from a spanwise slot is used to collect the turbulent boundary layer for a finite time and then release all of the flow instantaneously in one large eddy that convects downstream. Flow visualization and hot-film probe measurements are used together with pattern recognition algorithms to demonstrate the viability of the flow control method. A flat plate towed in a water channel is used as a test bed. The instantaneous velocity signal is used to compute important statistical quantities of the random velocity field, such as the mean, the root-mean-square, the spectral distribution, and the probability density function. When optimized for a given boundary layer, it is shown that the cyclic jet will produce periodic structures that are similar to the random, naturally occurring ones. These structures seem to trigger the onset of bursting events near the wall of the plate. Thus, the present device generates periodic structures in both the outer and inner regions of a turbulent boundary layer.

TABLE OF CONTENTS

1. INTRODUCTION

Short-wavelength laser propagation from an airborne platform is hampered by optical distortion caused by beam scattering as it passes through the aircraft boundary layer and shear layer flows. The scattering is mostly caused by the small-scale size of the turbulence in these regions (Chernov, 1967). The large-scale structures in the flow are random, and their arrival time at a particular point in the boundary layer is not a deterministic variable, making it very difficult to devise corrective measures for reducing or eliminating the optical distortion.

A typical airborne platform has a blunt turret that causes the flow to separate in its leeward side. At high subsonic Mach numbers, turbulence and flow separation result in a high level of density fluctuations which adversely affect the electromagnetic radiation transmitted from the aircraft. To improve the optical transmission quality of the flow field, the unsteadiness in the turbulent flow regions must be reduced by using passive or active flow control devices. de Jonckheere et al. (1982) conducted a wind tunnel experiment to quantify the beam degradation due to the flowfield around a cylinder-hemisphere body. Holographic interferometry and hot-wire anemometry were used to obtain the density fluctuations and turbulent correlation lengths in the shear layer. Their results, when incorporated into the optical propagation theory, predicted very low intensity in the farfield.

de Jonckheere and Chou (1982) developed scaling relationships to allow extrapolation of wind tunnel test results to full-scale flight conditions. In a later paper, de Jonckheere and Chou (1983) considered classical active flow control techniques including boundary layer suction and blowing. No net improvement in the optical transmission quality of the flow field was achieved. Moreover, the classical control methods represented an unacceptable level of power drain from the aircraft.

Smith et al. (1985) tested several fairing configurations surrounding the blunt turret. The passive fairings caused some reduction in the unsteadiness of the separated flow region behind the turret. While such passive flow control methods do not represent significant power drain, their overall effectiveness is perhaps limited. Innovative active flow control devices, with modest power requirements, are obviously needed for significantly improving the optical transmission quality of the flow field around the airborne platform.

By producing suitable periodic structures as the dominant feature of the flow field, the possibility of developing adaptive optics to compensate for the optical distortion is increased. The present investigation is aimed at exploring the feasibility of generating large-scale, periodic structures in a highly turbulent flow field. Two methods for altering the turbulence structure will be investigated. The first active flow control method is a cyclic, two-dimensional jet issuing from the wall of a boundary layer to collect the turbulence for a finite time and then release the collected fluid instantaneously in one large eddy that convects downstream once every period. The second method involves a turret-like device to divert the airplane's boundary layer away from the path of the laser beam. The resulting free shear layer will then be controlled by subharmonic perturbation. In the present paper, experiments were conducted using a flat plat towed in a water channel to test the first active control method. The control of the free shear layer using subharmonic perturbation will be the subject of a subsequent report.

The concept of large-eddy generation is detailed in Section 2. Description of the experimental setup is given in Section 3. Sections 4 through 8 contain the results of the flow visualization and fast-response velocity-probe measurements conducted to demonstrate the concept of artificial generation of large eddies in a turbulent boundary layer. Finally, a brief summary is presented in Section 9.

2. LARGE-EDDY GENERATING DEVICE

Two different ideas for generating and/or reinforcing the large-scale eddies in turbulent shear flows are sought. The first method will alter an existing turbulent boundary layer by creating larger eddies in a controlled manner. The second method uses a turret-like device to divert the laser beam away from the airplane's boundary layer. In its stead, a free shear layer of smaller thickness is formed and a means of controlling its eddies and dynamics is proposed. In the past, similar techniques have been shown to impose an element of control over the eddies within the flow field.

A large eddy generating device is sought for altering an existing turbulent boundary layer. In principle, the device would collect the turbulent fluid within the boundary layer for a finite time period and then release it instantaneously in one large eddy to pass downstream. Thus, during the collection period, the flow downstream of the device would be free of the existing turbulence. This period would be followed by the passage of one large eddy, and the cycle would then repeat itself.

An idealization of this concept, which utilizes a deformable airfoil, is illustrated in Figure 1. At the beginning of the cycle, the upper surface of the airfoil is presumed flush with the surface. At time $t > 0$, its leading edge rises above the turbulent boundary layer of thickness δ, but the trailing edge remains attached to the surface. Thus, the turbulent boundary layer is entrapped between the airfoil and the surface. As time progresses, the leading edge continues to rise, although at a decreasing rate, such that all of the incoming turbulent fluid is collected. Ideally, the airfoil would also deform, i.e., alter its camber, so that separation would not occur on the upper surface, hence ensuring a new, thin boundary layer at its trailing edge. As soon as the limits of the deformation are reached and separation is imminent, the airfoil would quickly resume its initial flush position, thus releasing all of the collected fluid.

One practical means of realizing the above idealized concept is to use a small, two-dimensional, cyclic jet as shown in Figure 2. The jet width d is typically much less than the boundary layer thickness, the jet spanwise length W is of the order of the laser beam diameter, and the jet velocity varies during the period P. As the fluid issues from the jet, the existing boundary layer will be entrapped and form a large eddy. Meanwhile, downstream a thinner boundary layer must result since it is deprived of much of its turbulence. In

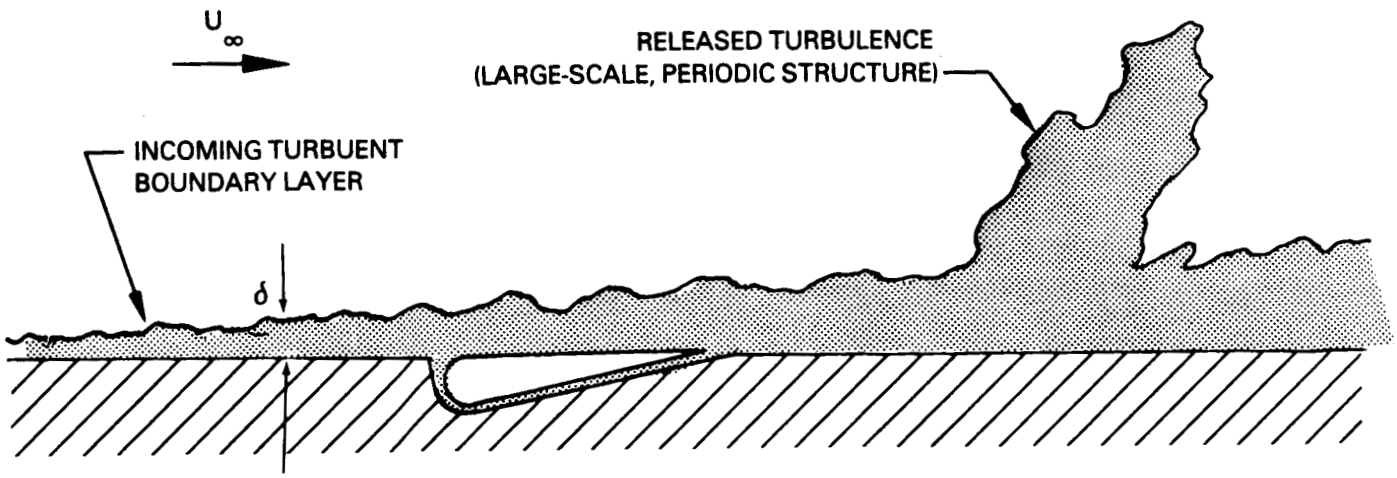

a. Beginning of Cycle. Airfoil Flush with Surface. The Generated Large Eddy from the Previous Cycle is seen Downstream

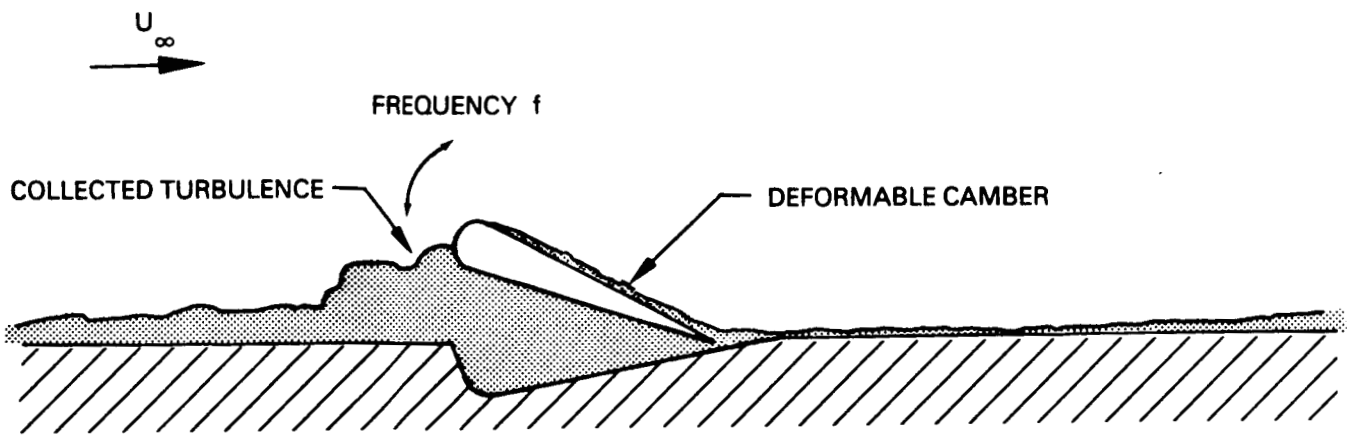

b. Airfoil at Mid-Cycle, with the Entrapped Turbulence

Figure 1. An Idealized Device for Generating Large Eddies

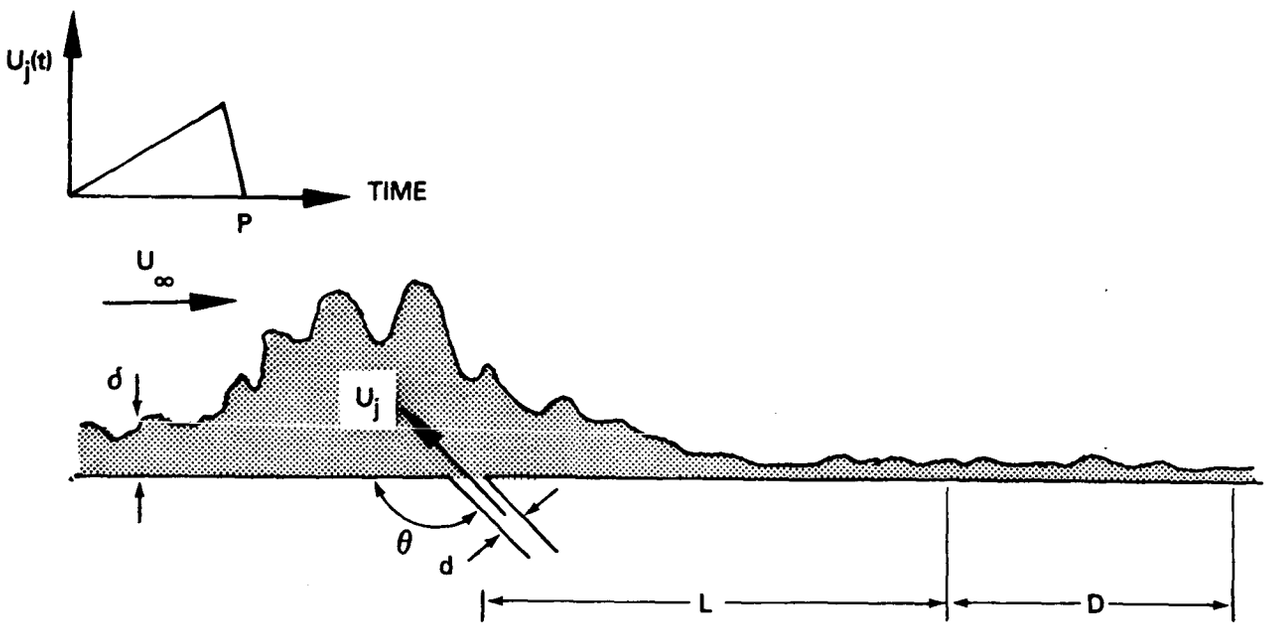

Figure 2. Large Eddy Generating Device Consisting of an Oscillating Jet of Fluid which Periodically Blocks the Normal Passage of the Turbulent Boundary Layer

the early stages of the cycle, the jet velocity could increase at a sufficient rate to contain most of the turbulence. Eventually, a point is reached where no further velocity increase is possible. The jet would be shut off immediately and the collected turbulence would be swept downstream as one large eddy and the cycle would begin again. Consequently, the protected area of size D downstream would have a very thin layer over it during most of the period, followed by the passage of one large eddy which is exactly periodic. This method could be further enhanced by using suction over part or all of the distance L in Figure 2. When phase locked with the pulsating jet, the suction could further reduce or eliminate the thin boundary layer during the period that the turbulence is being collected upstream by the jet.

Techniques similar to the method described above have been successfully used for generating and/or controlling the large eddies in turbulent boundary layers. Viets (1980) used an asymmetrical rotating cam embedded in the wall to produce large eddies in boundary layers with zero and adverse-pressure gradients. By using this device in a wide angle diffuser, Viets et al. (1981) were able to decrease the natural separation and improve the diffuser's performance. Alternatively, thin ribbons could be placed in the boundary layer and oscillated. Corke (1981) and Bushnell (1983) have shown that, at zero angle-of-attack without oscillation, a thin ribbon placed away from a flat plate and parallel to it leads to a reduction in the skin friction of the boundary layer. Corke (see his Figure 26) has also found that at negative attack angles, these devices enhance the large-eddy structure; thus, oscillating these devices in a pitching mode would suggest that a series of large and smaller eddies would be produced. However, it is felt that the pulsating jet has greater practical advantage because it is easier to control and has no external moving parts. In addition, by properly synchronizing the jet's amplitude, angle and acceleration, a great degree of controllability would appear to be achievable with the proposed jet. Similar developmental research by Gad-el-Hak and Blackwelder (1985; 1986a; 1986b) has led to a pulsating jet device that controls the formation and growth of the large bound vortices on delta wings and similar lifting surfaces.

The second method of interfering with the boundary layer on the plate is to divert it away from the path of the laser beam as illustrated in Figure 3. An aerodynamic window (Russell, 1974; Christiansen et al., 1975) may be contained inside the turret-like device shown in the figure. It is assumed

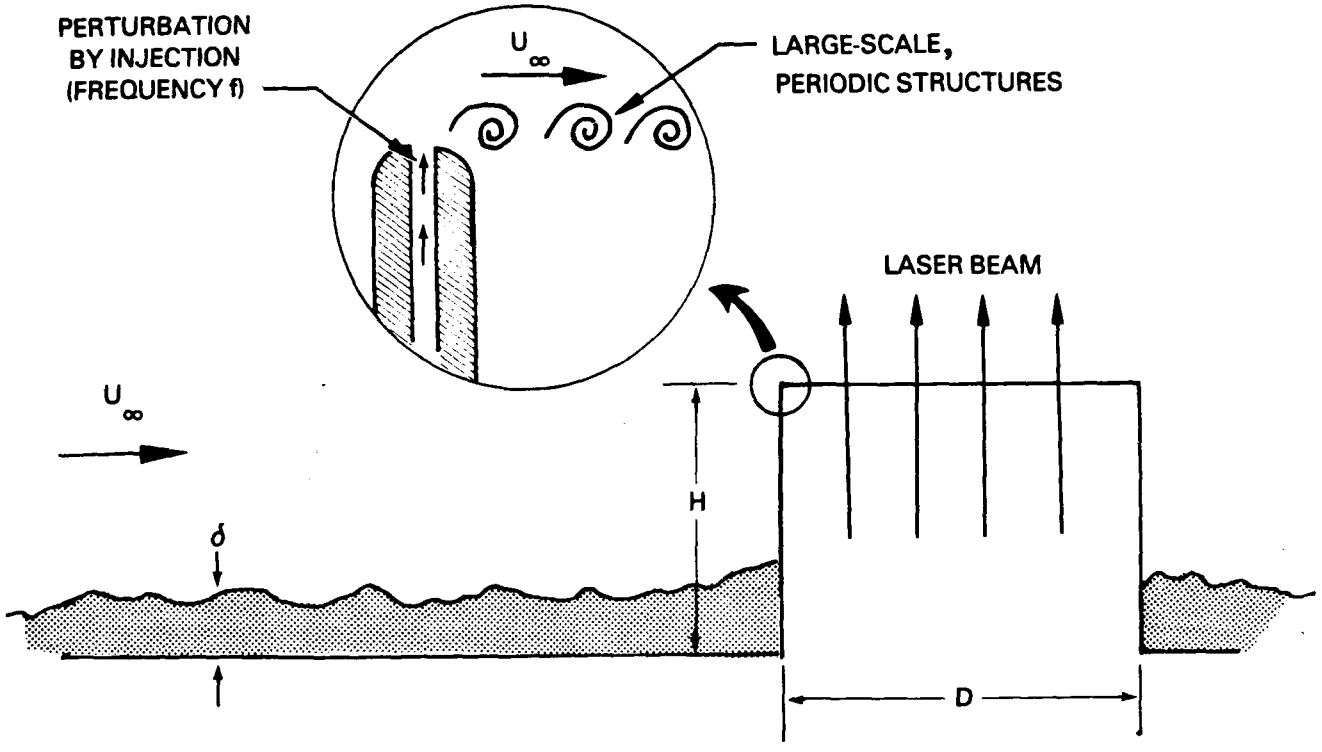

Figure 3. A Diversion Fairing Used to Divert the Laser Beam Away from the Airplane's Boundary Layer. The Insert Shows a Small Perturbation Introduced at the Lip of the Fairing to Control the Resulting Free Shear Layer

that a region of size D is to be protected from the normal boundary layer so that radiation emitted through this region will not suffer distortion by the turbulence. Thus, a fairing of height H, which is larger than the boundary layer thickness δ, is erected around the region D. This forces the boundary layer to pass by the side of the turret-like device, thus providing an undisturbed path for the laser beam. Although the boundary layer is eliminated from the problem, a turbulent free shear layer will be formed at the lip of the fairing, thus providing another source of distortion. However, this free shear layer can perhaps be readily controlled, as described below.

In an uncontrolled environment, Brown and Roshko (1971; 1974) have shown that a free shear layer flow consists of vortical eddies having length scales comparable to the layer thickness. Winant and Browand (1974) further showed that these eddies form by an amalgamation process called pairing, which usually consists of the merging of two neighboring eddies to form a single larger eddy. Ho and Huang (1982) have shown that whenever a subharmonic perturbation is added to the flow field, amalgamations of 3,4,...,10 vortices can be accomplished during one cycle, which leaves a more stable flow field consisting of larger vortices that are relatively inactive; i.e. they do not participate in any further amalgamations for a considerable distance downstream. Oster et al. (1978) used this method to generate and control the eddies formed behind a splitter plate in a mixing layer.

To control the growth and development of the mixing layer forming at the top of the proposed diversion-fairing device, a subharmonic disturbance may be introduced at the lip of the fairing. The results of Oster et al. (1978) indicate that eddies of size U_∞/f (where f is the forcing frequency) can be generated over a fairly broad range of frequencies. Also, Ho & Huerre (1984) have shown that a mixing layer can be controlled even in the presence of a noisy background by simply increasing the amplitude of the subharmonic perturbation. Thus, large-scale, periodic structures may be artificially generated in the free shear layer at the lip of the diversion fairing. These structures will replace the random ones occurring naturally. A laser beam radiating out of the turret-like device will encounter a series of periodic structures as the dominant feature of the flow field, and the possibility of developing adaptive optics to compensate for these organized structures is then greatly increased.

One possible problem with the diversion-fairing device applied to an airborne platform would be its directional sensitivity. Whenever the airplane changes its direction of motion, the free shear layer flow and its natural shedding frequency would change. This will make it difficult to control the periodicity of the large-scale structures. However, by adding a small splitter plate at the top of the turret-like structure, its directional sensitivity will be greatly reduced. A second important issue is the three-dimensionality of the free shear flow under consideration. In contrast to two-dimensional and axially-symmetric flows, perturbing such a complex three-dimensional flow may not be straightforward and very little is available in the open literature on how to handle the additional complications introduced by the geometry. Some research along these lines is obviously needed.

In the present paper, only the first method of artificially generating large eddies in a turbulent boundary layer is considered. The control of the free shear layer using subharmonic perturbations will be the subject of a subsequent report.

3. EXPERIMENTAL APPROACH

3.1 Towing Tank

Turbulent and laminar boundary layers were generated by towing a flat plate in a water channel that is 18 meters long, 1.2 meters wide and 0.9 meter deep. The towing tank, shown in Figure 4, has been described by Gad-el-Hak et al. (1981) and Gad-el-Hak (1986c). The flat plate was rigidly mounted under a carriage that rides on two tracks mounted on top of the tank. During towing, the carriage was supported by an oil film to ensure a vibrationless tow, having an equivalent freestream turbulence of about 0.1 percent. The carriage was towed by two cables driven through a reduction gear by a 1.5-hp Boston Ratiotrol motor. The towing speed was regulated within an accuracy of 0.1 percent. The system was able to achieve towing speeds between 5 and 140 cm/s for the present study. However, most of the runs reported here were conducted at a speed of 20 cm/s.

3.2 Flat Plate

A unique, zero-pressure-gradient flat plate was constructed for the present investigation. The 1-meter by 2-meter structure, shown in Figure 5, is made of glass-reinforced polycarbonate plate 6 mm thick, glued to a stainless steel frame designed for minimum obstruction to the flow. The plate has an elliptic nose at the leading edge and an adjustable lifting flap at the trailing edge. To avoid leading-edge separation and premature transition, the flap is adjusted so that the stagnation line near the leading edge is located on the working surface of the plate. The plate's smooth surface and flatness to within a few microns make it one of the most controlled test beds available for boundary layer research. A laminar boundary layer can be obtained over the entire working surface for towing speeds in the range of 5 to 80 cm/s. Trips are used to generate a fully developed turbulent boundary layer. The trips are brass cylinders 0.32 cm in diameter and 0.25 cm high placed 5 cm downstream of the leading edge and having their axes perpendicular to the flat plate.

3.3 Large-Eddy Generating Device

The large-eddy generating device considered in the present investigation consists of a two-dimensional, spanwise, cyclic jet, shown schematically in

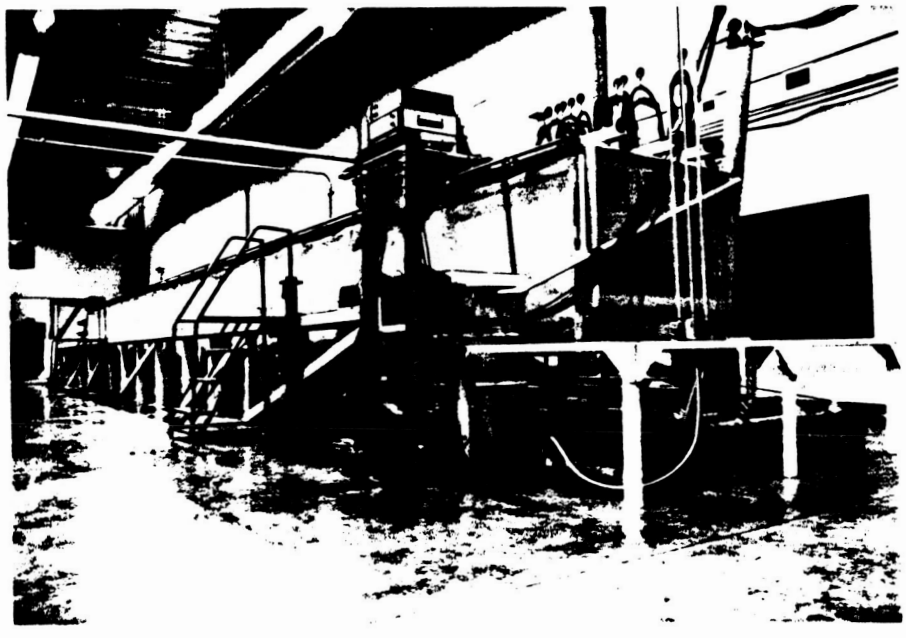

Figure 4. Flow Research 18-Meter Towing Tank

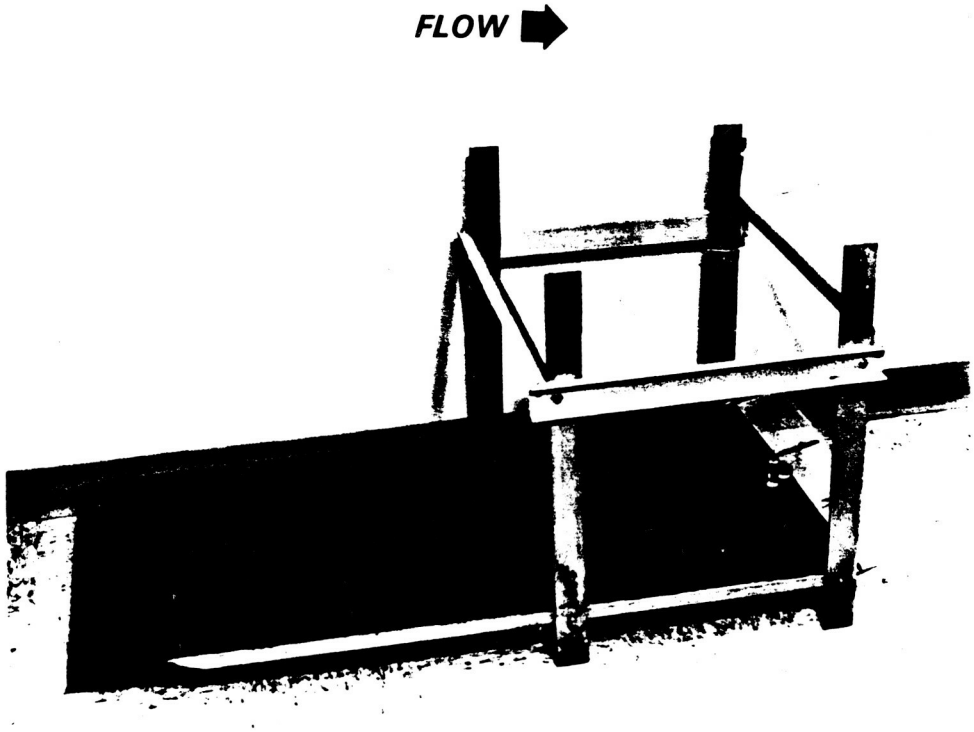

Figure 5. Photograph of the Zero-Pressure-Gradient Flat Plate

Figure 2. As mentioned in Section 2, the periodic jet is used to collect the turbulent boundary layer for a finite time and then release all of the flow instantaneously in one large eddy that convects downstream. The primary parameters of this jet are its physical size d and W; amplitude of velocity U_j; frequency f; angle Θ; and acceleration of jet velocity dU_j/dt. The width of the jet d is dictated by the boundary layer thickness, i.e., the jet must be smaller than the boundary thickness δ. Its spanwise width W is determined by the laser beam diameter. The other four parameters are clearly interrelated and cannot necessarily be examined independently. Nevertheless some guidelines and ranges can be established; e.g., the frequency f of the artificial perturbation should match the mean frequency of the naturally occurring large-eddy structures. Therefore, f must be of order U_∞/δ (Kovasznay et al., 1970). The initial range of exploration uses a velocity amplitude of the order of U_∞ and a reduced (or nondimensional) jet frequency in the range of $0.1 \leq f\delta/U_\infty \leq 1.0$. The jet angle Θ is greater than 90° as defined in Figure 2; thus, several angles in this range should be explored. In the initial phase of this investigation, this angle was fixed at $\Theta = 135°$. The optimum acceleration (i.e. temporal variation of the jet velocity) may not necessarily be sinusoidal; consequently, forward and rearward facing ramp functions, triangular functions, etc., should be explored.

To accomplish the desired degree of control of the cyclic jet, the system shown schematically in Figure 6 was used. The laboratory's air supply was used to pressurize a stainless-steel tank containing water. The flow rate of the secondary fluid was controlled by using a pressure regulator for the air's supply line and a ball valve driven by a stepping motor for the secondary fluid's conduit. The duty cycle of the valve was controlled within the limitations of the experimental apparatus using an APPLE II microcomputer. For example, a slow opening followed by fast closing, a symmetric cycle followed by a given delay before the starting of a new cycle, etc. The controlled secondary flow passed through a small conduit to an internal reservoir directly behind a 1-mm-wide, 15-cm-long slot that was built into the flat plate. This reservoir ensured that the ejection speed was uniform to within 2 percent along the entire spanwise slot. The slot was located at x = 62 cm downstream of the plate's leading edge.

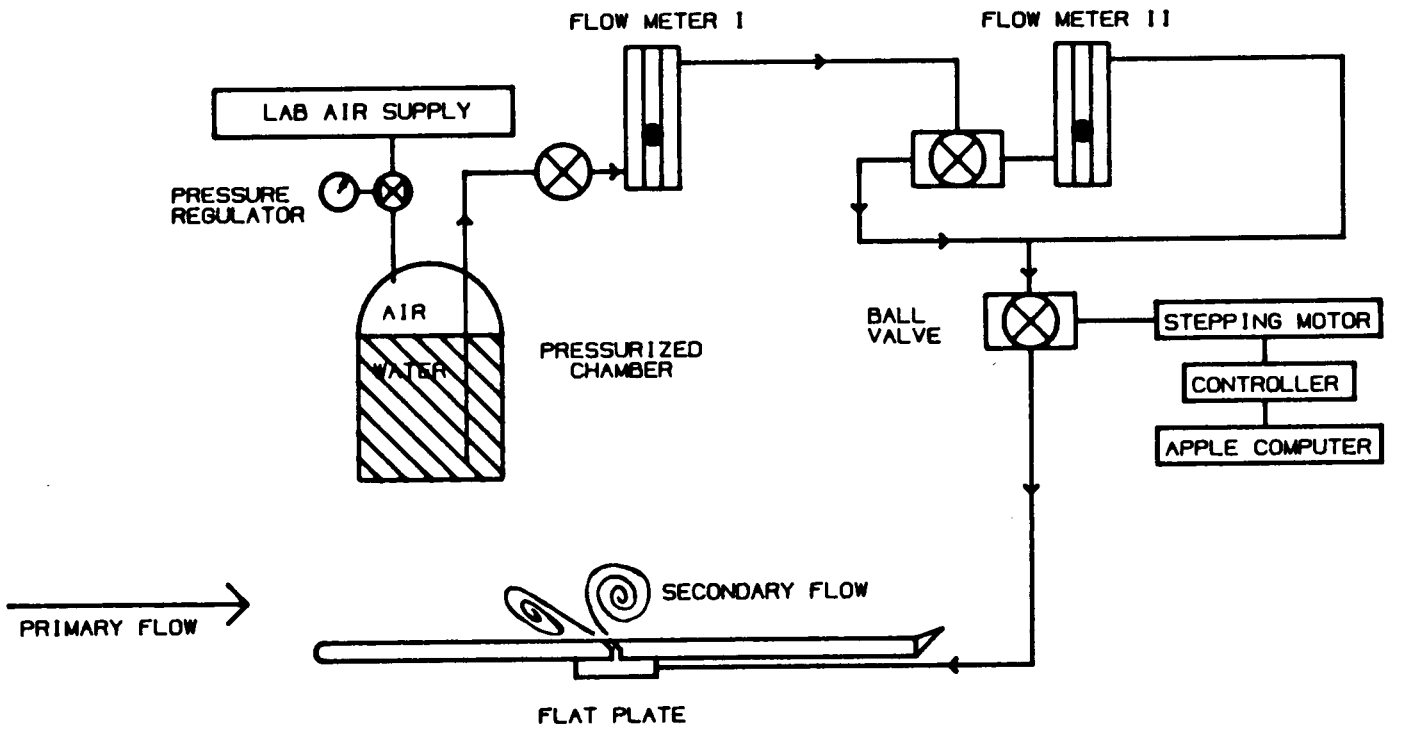

Figure 6. Schematic of the Large Eddy Generating Device

3.4 Visualization Methods

To visualize the large eddies and near-wall events in the natural and perturbed turbulent boundary layers, both fluorescent dye and hydrogen-bubble techniques were used (Gad-el-Hak, 1986a; 1986b). The dyes were seeped into the boundary layer through a spanwise slot 0.15 mm wide and 15 cm long and located 77 cm downstream of the leading edge of the flat plate. The dye slot was milled at a 45° angle inclined toward the plate's trailing edge to minimize the flow disturbance. Dye was also introduced into the primary flow by mixing minute amounts of fluorescent dye with the secondary fluid in the pressure tank. The hydrogen bubbles were generated using a stainless-steel wire having a diameter of 50 microns and a length of 10 cm. The wire was placed at different locations either parallel to or perpendicular to the flat plate to obtain top views or side views, respectively, of the flow field. To create time lines, a standard circuit was employed to supply intermittently 100 volts to the wire, which acted as a cathode.

Both the fluorescent dyes and the hydrogen bubbles were illuminated using a sheet of laser light projected in the desired plane. This provided an extra degree of freedom in observing the large-eddy structures and the bursting events, because both the tracer and the light location could be controlled within the limitations of the experimental apparatus. In order to generate a sheet of light, a 5-watt argon-ion laser (Spectra Physics Model 164) was used with a mirror mounted on an optical scanner having a natural frequency of 720 Hz (General Scanning, Inc.) and driven by a sine-wave signal generator of the desired frequency. The frequency of the sine wave was usually set equal to the inverse of the shutter speed of the camera. The light sheets were approximately 1 mm thick, which was sufficient to resolve the large structure within the turbulent regions. A vertical sheet of laser light parallel to the flow was used to visualize side views of the large-eddy structures, and a horizontal sheet near the surface of the plate was used to obtain top views of the flow field.

3.5 Velocity Measurements

Miniature boundary-layer hot-film probes (TSI Model 1260) were used in the present investigation to measure the longitudinal mean and fluctuating velocities. The probe diameters were 0.025 mm, and their sensing lengths were 0.25 mm. A probe traverse powered by a stepping motor and controlled through

an APPLE II microcomputer was used for surveying the boundary layers. Conventional statistical quantities, such as the mean, the root mean square, the spectral distribution, the autocorrelation coefficient, and the probability density function, were computed from the velocity signals.

3.6 Pattern-Recognition Algorithms

The purpose of the present investigation is to determine the effectiveness of the periodic injection of secondary fluid on the large-eddy structures that dominate the outer portions of a turbulent boundary layer. However, the initial visualization experiments indicated that the artificial eddies affect the low-speed streaks and bursting events that occur very near the wall. To further investigate this important finding, two pattern-recognition algorithms were used to more objectively detect low-speed streaks and bursts.

A novel pattern-recognition technique that utilizes the streamwise velocity signal from three hot-film probes was developed to detect low-speed streaks (Gad-el-Hak et al., 1984). The probes were located at $y^+ = 10$ at the same streamwise position with a spanwise separation of approximately 20 ν/u_τ. Thus, the total array spanned 40 ν/u_τ, which is approximately half the average low-speed streak spacing. A pattern recognition algorithm identified a low-speed region whenever all three signals were less than the local mean velocity by one-half the root-mean-square (rms) value, and the velocity measured by the middle probe was less than the velocity on either side. The beginning and end of each low-speed region could thus be identified, and the streaks' average length and frequency computed.

To test this algorithm, experiments were first carried out using a rake of twelve velocity probes located at $y^+ = 10$ but having a significantly broader spanwise extent. Low-speed streaks were readily identified using the isovelocity contours computed from the rake's output, and their spacing was in reasonable agreement with results obtained from visualization experiments conducted under similar conditions. The results of the algorithm were compared with the low-speed streaks obtained from the rake. The comparison showed that the detected algorithm picked out the streaks exceedingly well, and that the streaks meander in the spanwise direction so that often a single streak crosses the probes two or more times, resulting in multiple detections.

The second pattern-recognition algorithm employed in the present investigation was a burst detection scheme using the variable-interval time-averaging (VITA) technique developed by Blackwelder & Kaplan (1976). A single hot-film probe located at $y^+ = 20$ was used for burst detection. The program counted the number of bursts that occur near the wall and recorded their intensities.

4. PERIODIC INJECTION IN THE ABSENCE OF BOUNDARY-LAYER FLOW

The flow rate from the cyclic spanwise slot was controlled using the pressure regulator and the ball valve shown schematically in Figure 6. A typical example of the ejection of water, mixed with fluorescent dye, in the absence of boundary-layer flow (the flat plate was held stationary in the water channel) is shown in the photographs in Figure 7. A vertical sheet of laser light perpendicular to the spanwise slot illuminated the dyed fluid issuing from the slot. The flow speed increased linearly from 0 to 45 cm/s at an acceleration rate of 150 cm/s^2 (total acceleration time = 0.3 s), followed by a deceleration from 45 to 0 cm/s at a rate of 450 cm/s^2 (total deceleration time = 0.1 s). The leading edge of the flat plate is located to the left of the side view shown in the figure, and the time in seconds measured from the starting cycle is shown under each photograph. It is clear that the secondary flow forms a clockwise-rotating vortex as it comes out of the 45° sharp-leading-edge slot. The presence of the wall of the flat plate influences the evolution of this vortex. The maximum injection speed, the acceleration rate, and the deceleration rate also affect the flow from the spanwise slot.

The instantaneous injection velocity of the cyclic jet can be recorded by placing a hot-film probe just outside the spanwise slot. Typical time record is shown in Figure 8 for a periodic injection having maximum injection speed of 140 cm/s, acceleration rate of 350 cm/s^2 and deceleration rate of 560 cm/s^2. The sensitive element of the hot-film probe was placed parallel to the spanwise slot at a distance of 0.5 mm (0.5d) from the two-dimensional orifice. It is clear from the 15 injection cycles shown in Figure 8 that excellent repeatability is achieved.

A closeup of the same run is repeated in Figure 9a for three injection cycles. The flow from the slot is clearly turbulent. At lower maximum injection speed, the flow is less turbulent as shown in Figure 9b. In the latter case, the duty cycle of the ball valve was symmetric and both the acceleration and deceleration rates were 667 cm/s^2. A larger delay between successive cycles was also programmed in this case.

In summary, the flow rate from the spanwise slot can be controlled within the limitations of the experimental apparatus. The maximum injection speed, the acceleration and deceleration rates, and the delay time between successive cycles can be changed to optimize the simulation of large-eddy structures in a given turbulent boundary layer.

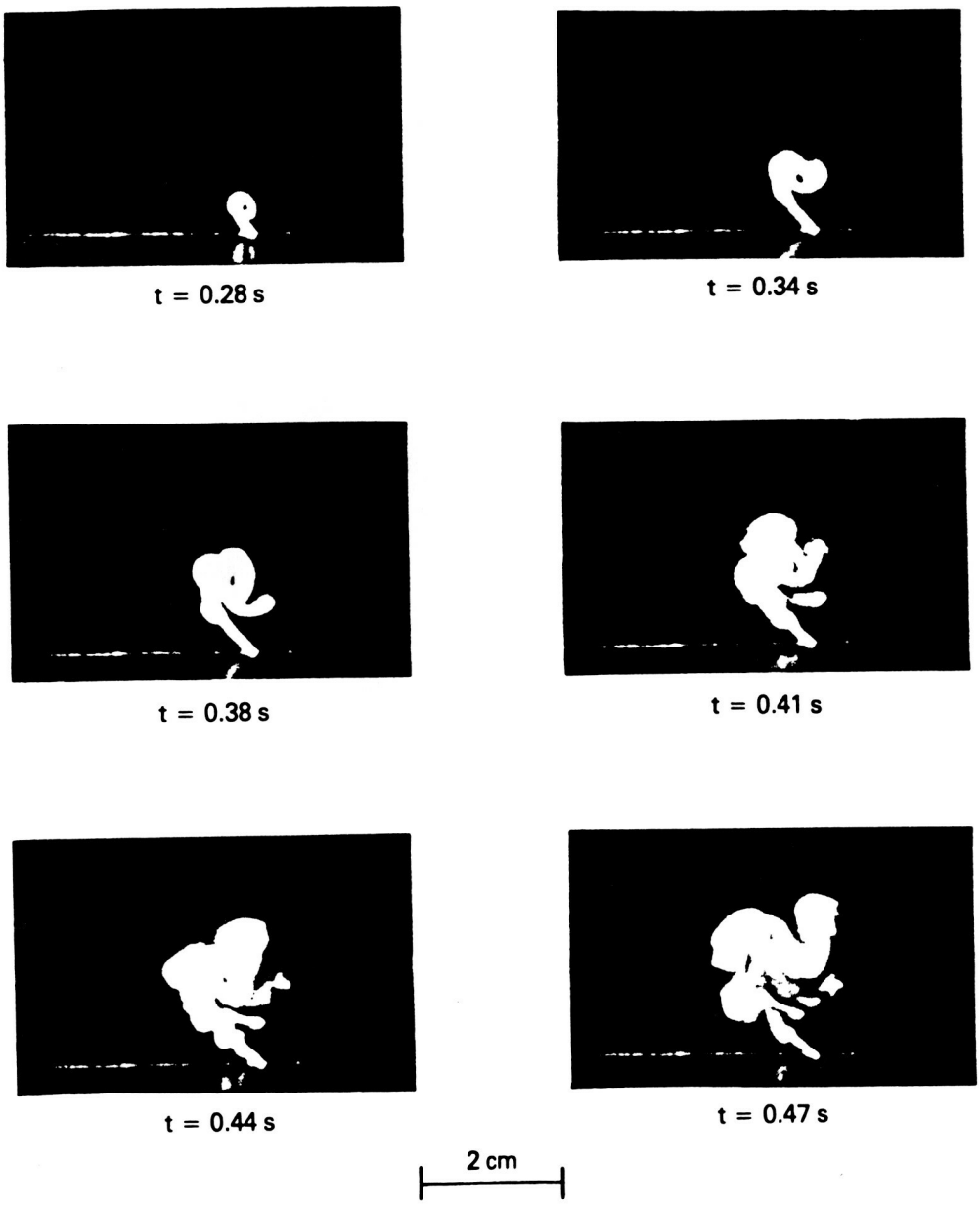

Figure 7. Periodic Injection from Spanwise Slot. Flat Plate is Stationary and Maximum Injection Speed = 45 cm/s

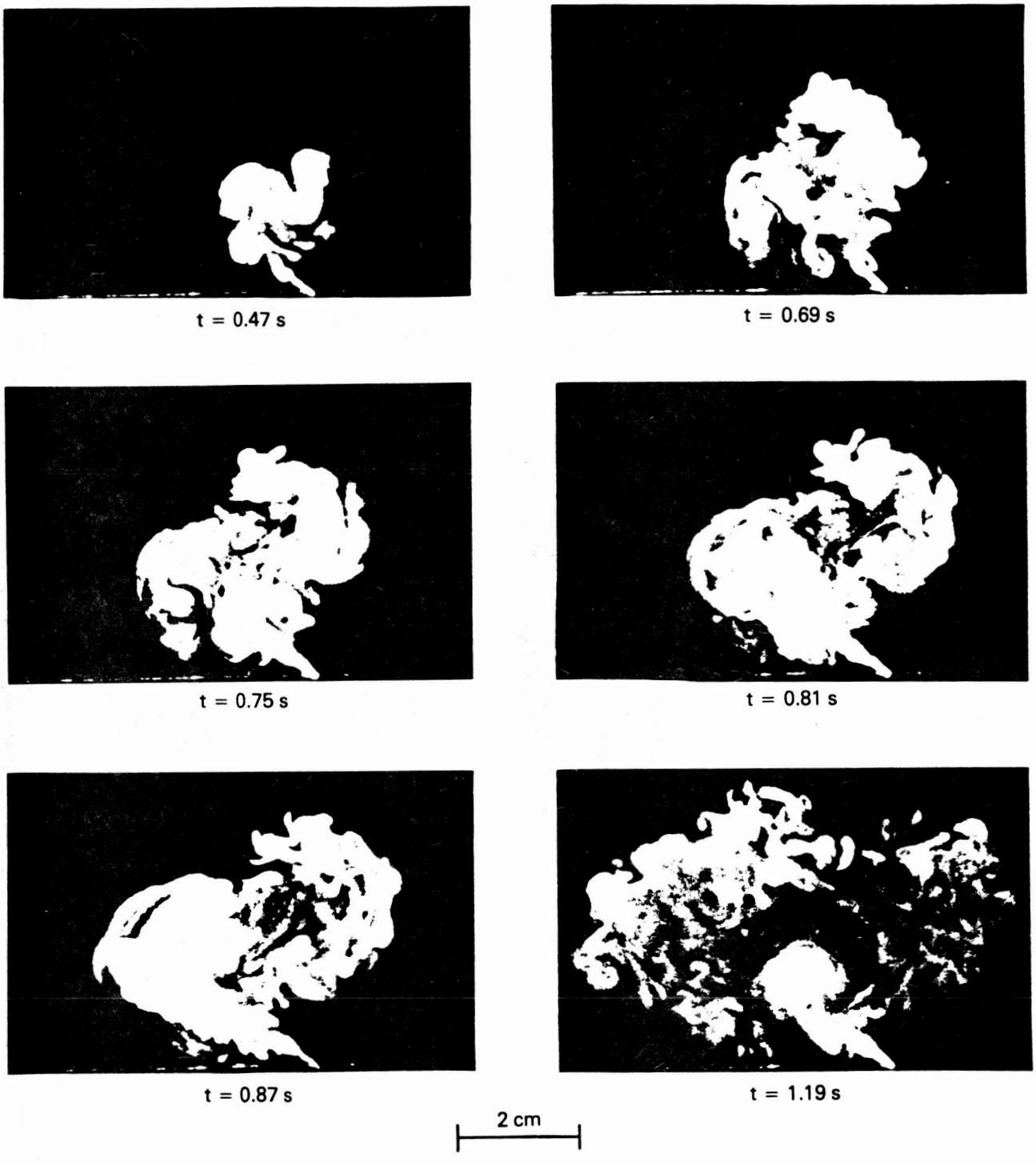

Figure 7. Periodic Injection from Spanwise Slot. Flat Plate is Stationary and Maximum Injection Speed = 45 cm/s (Cont.)

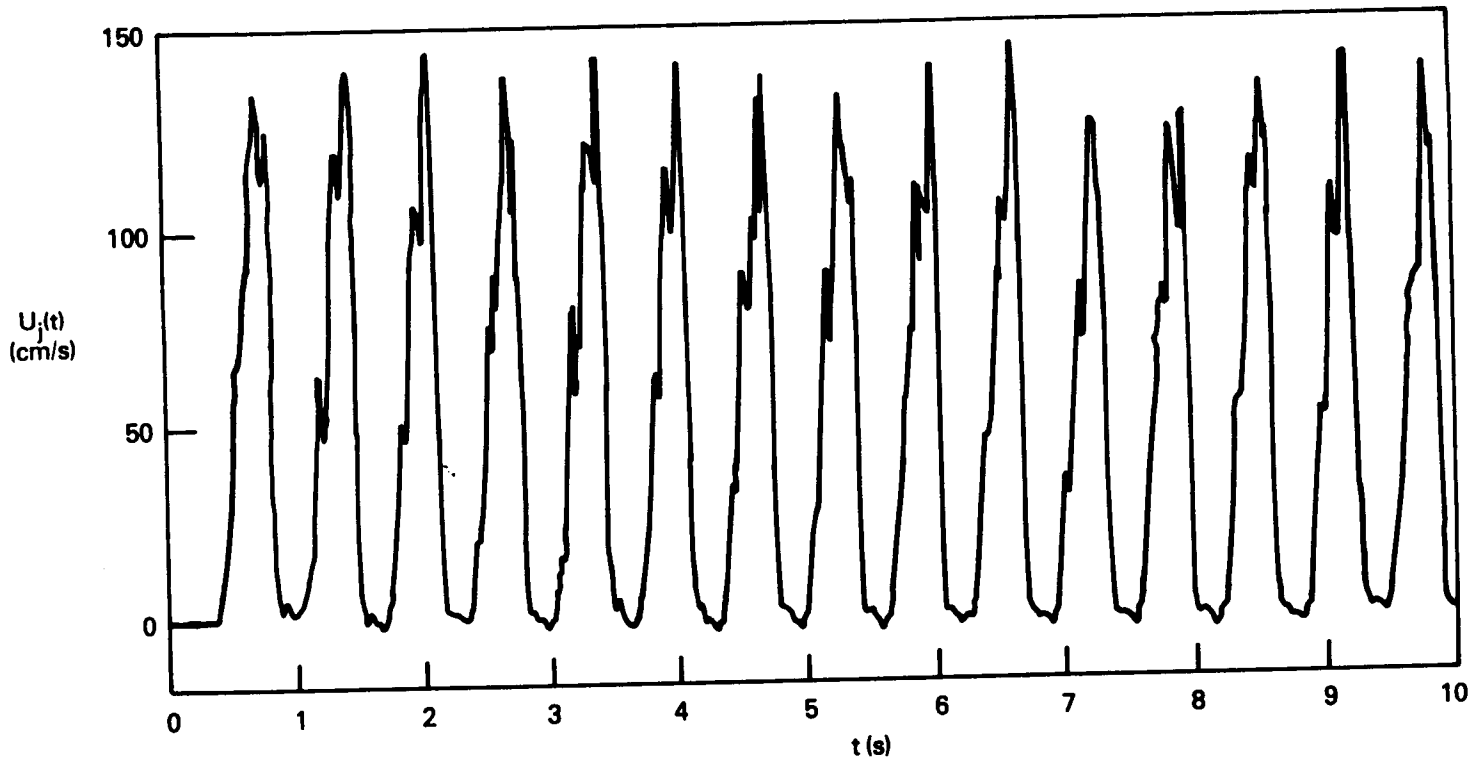

Figure 8. Periodic Injection of Secondary Fluid from Spanwise Slot. Instantaneous Injection Velocity. Time ON = 0.4 s; Time OFF = 0.25 s; Maximum Injection Speed = 140 cm/s

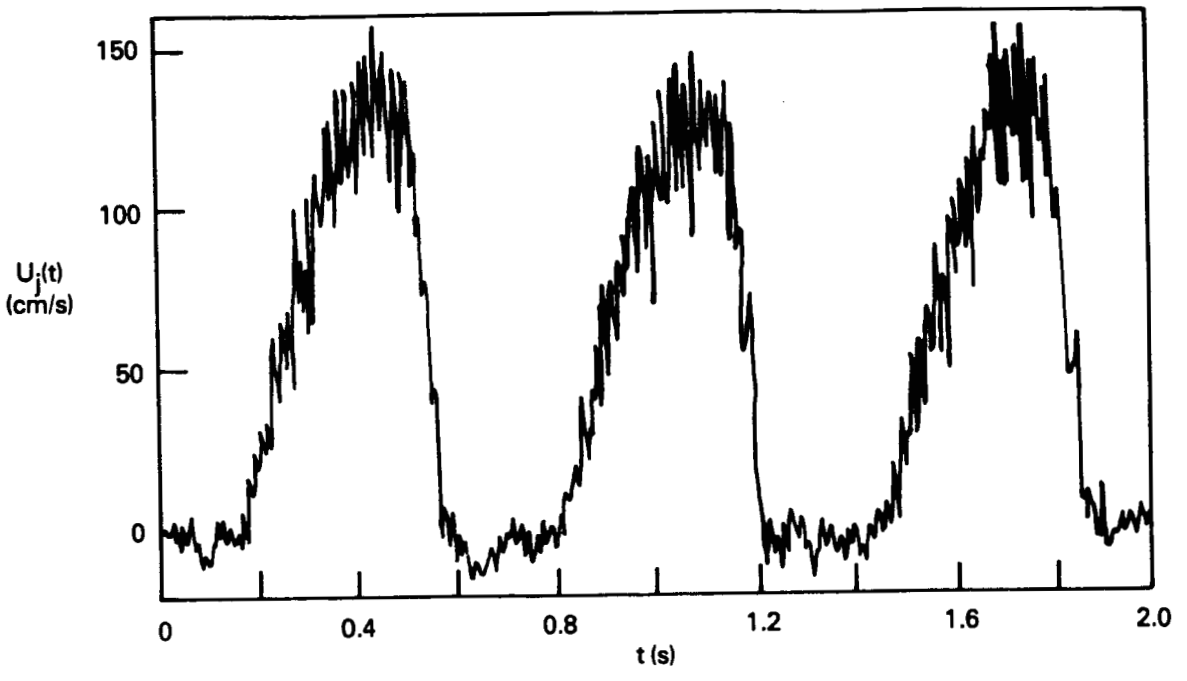

a. Time ON = 0.4 s; Time OFF = 0.25 s; Maximum Injection Speed = 140 cm/s

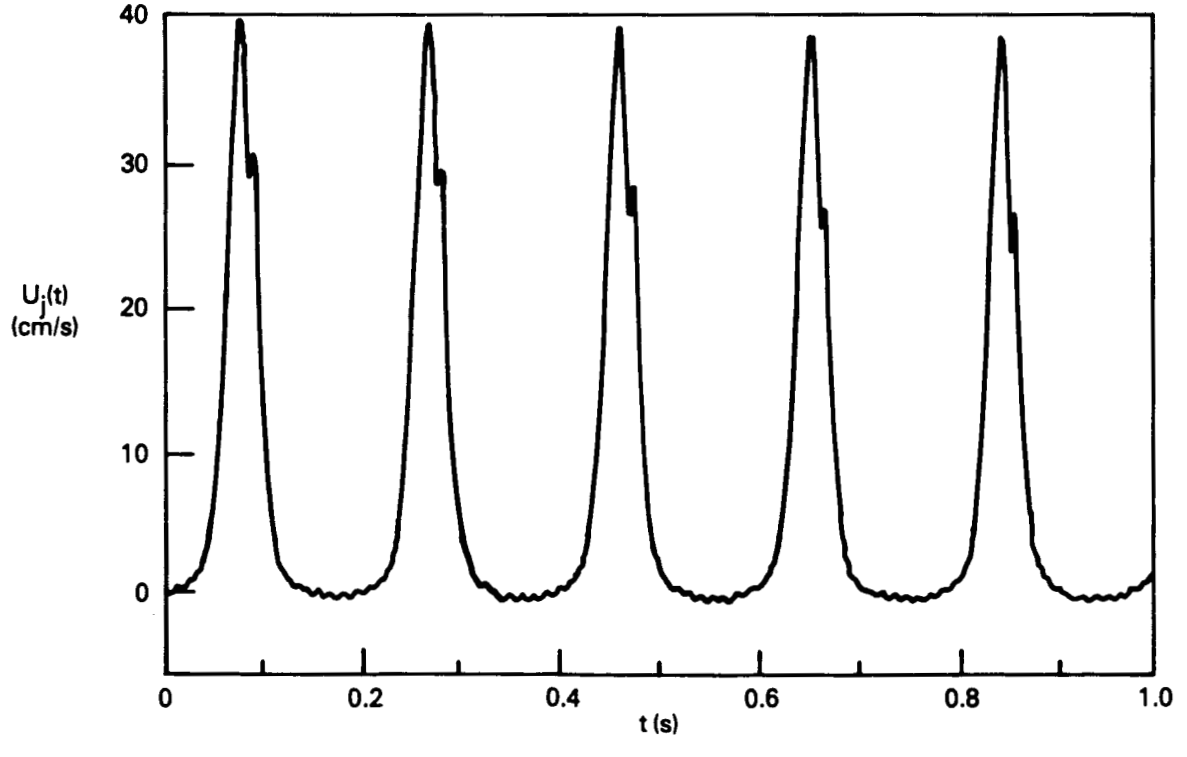

b. Time ON = 0.06 s; Time OFF = 0.13 s; Maximum Injection Speed = 40 cm/s

Figure 9. Instantaneous Injection Velocity from Spanwise Slot

5. PERIODIC INJECTION INTO A TURBULENT BOUNDARY LAYER

The aim of the present investigation is to develop a method of artificially generating large-scale, periodic structures in a turbulent shear flow. To test whether or not these artificial structures simulate the random, naturally occurring ones, flow visualization and fast-response probe measurements were conducted.

At a freestream speed of 20 cm/s and at the two stations considered in the present investigation x = 67 cm and x = 100 cm, the momentum thickness Reynolds numbers were R_θ = 455 and 632, and the displacement thickness Reynolds numbers were $R_{\delta*}$ = 585 and 813, respectively. The mean and root-mean-square longitudinal velocity profiles of the turbulent boundary layer agreed well with those for the zero-pressure-gradient flat plate (Purtell, et al., 1981). The mean profiles always had well-defined linear, logarithmic and wake regions.

In the presence of a turbulent boundary layer, the periodic injection from the spanwise slot was visualized using a vertical sheet of laser light parallel to the freestream direction. In Figure 10, the turbulent boundary layer flow was from left to right and the secondary fluid from the slot was premixed with minute amounts of fluorescent dye. The flow was visualized just downstream of the injection slot. The parameters for the periodic injection were: maximum injection speed = 20 cm/s, acceleration rate = 50 cm/s^2, and deceleration rate = 80 cm/s^2. The freestream speed was U_∞ = 20 cm/s, and the time in seconds from the start of a typical cycle is indicated under each photograph. As shown in the figure, large-eddy-like structures are formed downstream of the spanwise slot. The shear flow in the boundary layer interacts in a unique way with the clockwise-rotating vortex issued periodically from the slot to form the structures marked by the dye. These structures stretch while convecting downstream. Two consecutive structures are separated by a distance that depends on the ratio of the injection speed to the freestream speed and on the reduced jet frequency $f\delta/U_\infty$. In the present example, the maximum injection speed is equal to the freestream speed and the nondimensional frequency is 0.18.

An apparently different large-eddy structure is artificially generated when the reduced jet frequency is increased, as shown in Figure 11. In this case, the freestream speed and the maximum injection speed are the same as the case depicted in Figure 10, but the acceleration and deceleration rates are increased such that the reduced frequency is increased three folds to

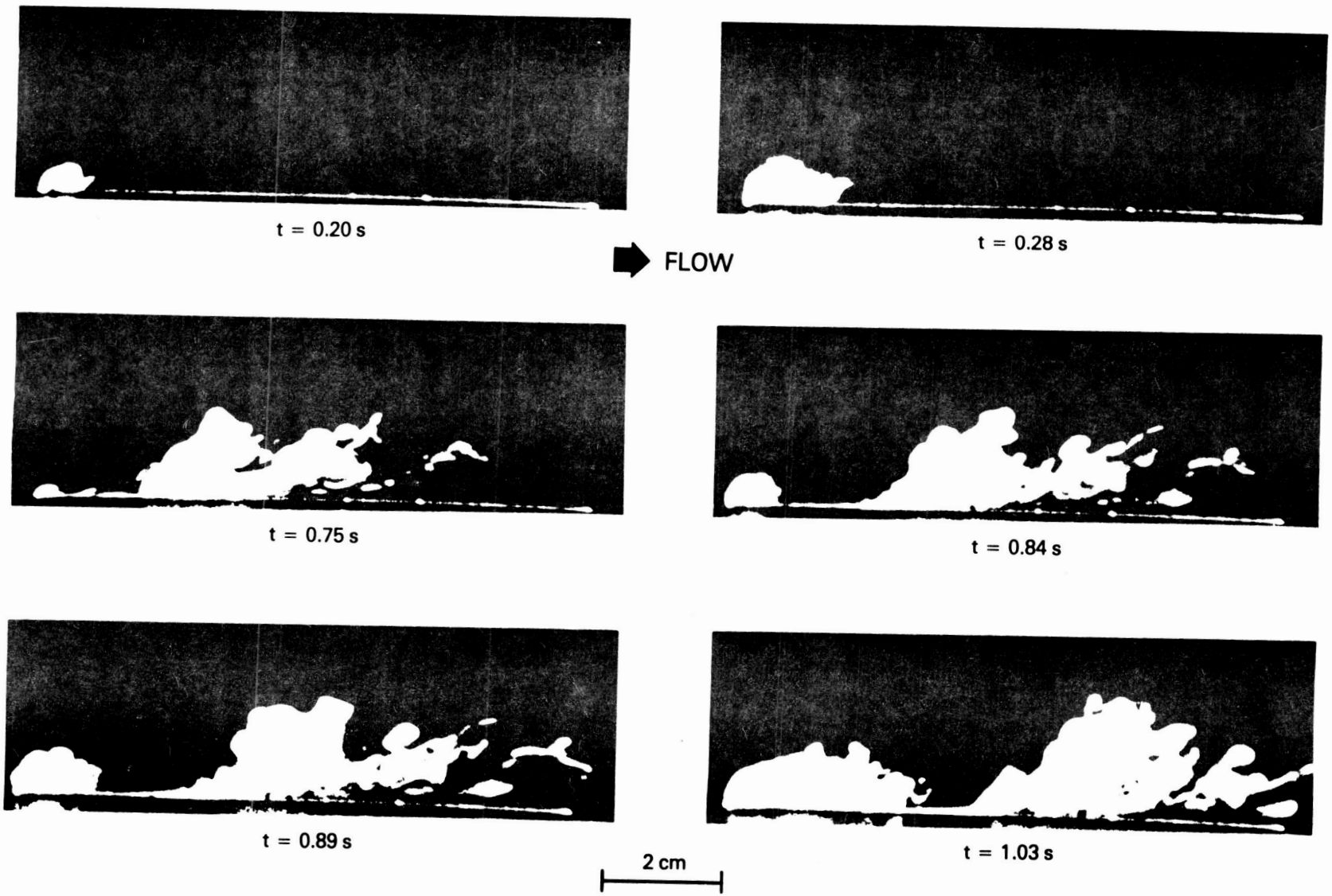

Figure 10. Periodic Injection into a Turbulent Boundary Layer. U_∞ = 20 cm/s; Maximum Injection Speed = 20 cm/s; Time ON = 0.40 s; Time OFF = 0.25 s

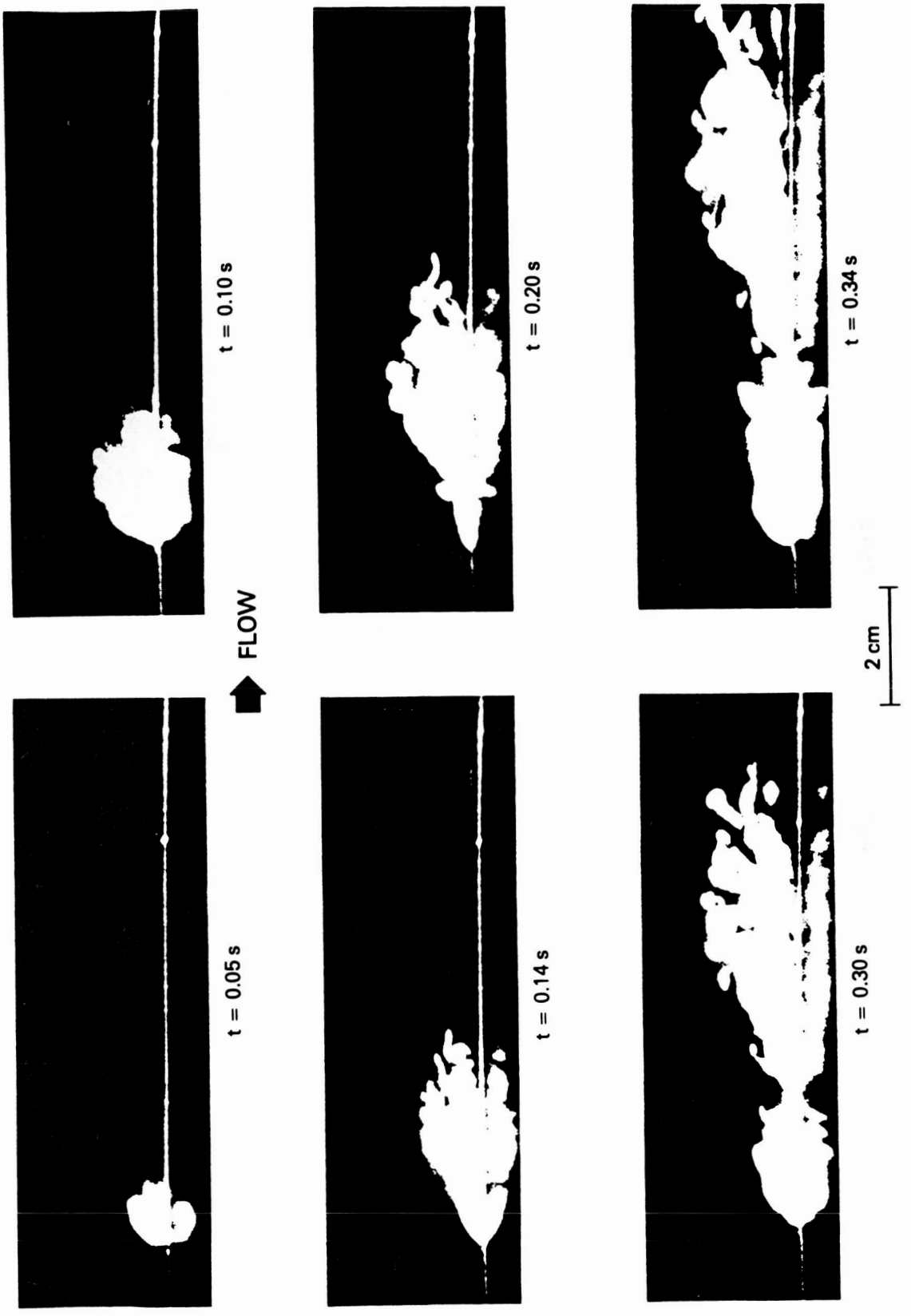

Figure 11. Periodic Injection into a Turbulent Boundary Layer. U_∞ = 20 cm/s; Maximum Injection Speed = 20 cm/s; Time ON = 0.1 s; Time OFF = 0.1 s

$f\delta/U_\infty$ = 0.58. The duty cycle of the ball valve is asymmetric in the run depicted in Figure 10 (opening time = 0.4 s, and closing time = 0.25 s), while it is symmetric in the case shown in Figure 11 (opening time = closing time = 0.1 s). The two consecutive eddies are closer to each other in the latter case.

A different perspective of the flow field is achieved by dying both the incoming turbulent boundary layer flow as well as the cyclic, secondary fluid from the spanwise slot. In Figure 12, a dark yellow dye is introduced upstream of the injection slot near the leading edge of the plate, and a lighter color dye marks the periodic flow from the spanwise slot. The natural, random large-eddy structures are visualized in the first photograph at t = 0 (origin of time coincides with the start of the cyclical injection). A periodic jet is introduced into the natural boundary layer such that the maximum injection speed = U_∞ = 20 cm/s and the reduced frequency $f\delta/U_\infty$ = 0.1. An interesting phenomenon is associated with this relatively slow injection of secondary fluid. At the end of the opening cycle (fourth frame in Figure 12 at t = 1.05 s), the injected fluid reaches approximately the same height as that of the natural boundary layer. However, at t = 1.45 s (last frame in Figure 12), the interaction between the natural and artificial eddies results in the large intrusion of the lighter dye into the potential flow region. The thickness of this region is almost twice that of the natural boundary layer thickness.

Hot-film probes were used in the present investigation to record the instantaneous streamwise velocity components. Three such records are depicted in Figure 13 for the natural and perturbed turbulent boundary layers. The free- stream speed in all three runs was U_∞ = 20 cm/s, and the probe was located at x = 100 cm. At y/δ = 0.6, the natural boundary layer has a mean velocity of 17.92 cm/s and the typical random fluctuations shown in the top record in the figure. When the probe is raised to y/δ = 0.8, the mean velocity is increased to 19.21 cm/s and the negative spikes (marked by the arrows in the middle record) indicate the passing of natural, large-eddy structures by the fixed probe position. These eddies occur at random but have a mean frequency of about 0.8 Hz. When secondary fluid is introduced from the spanwise slot at a period corresponding to the mean natural period, the velocity records shown in the bottom of Figure 13 result. Note that the hot-film probe is located 38 cm (12δ) downstream of the injection slot, yet the negative spikes resulting from the passing of the artificial eddies by the

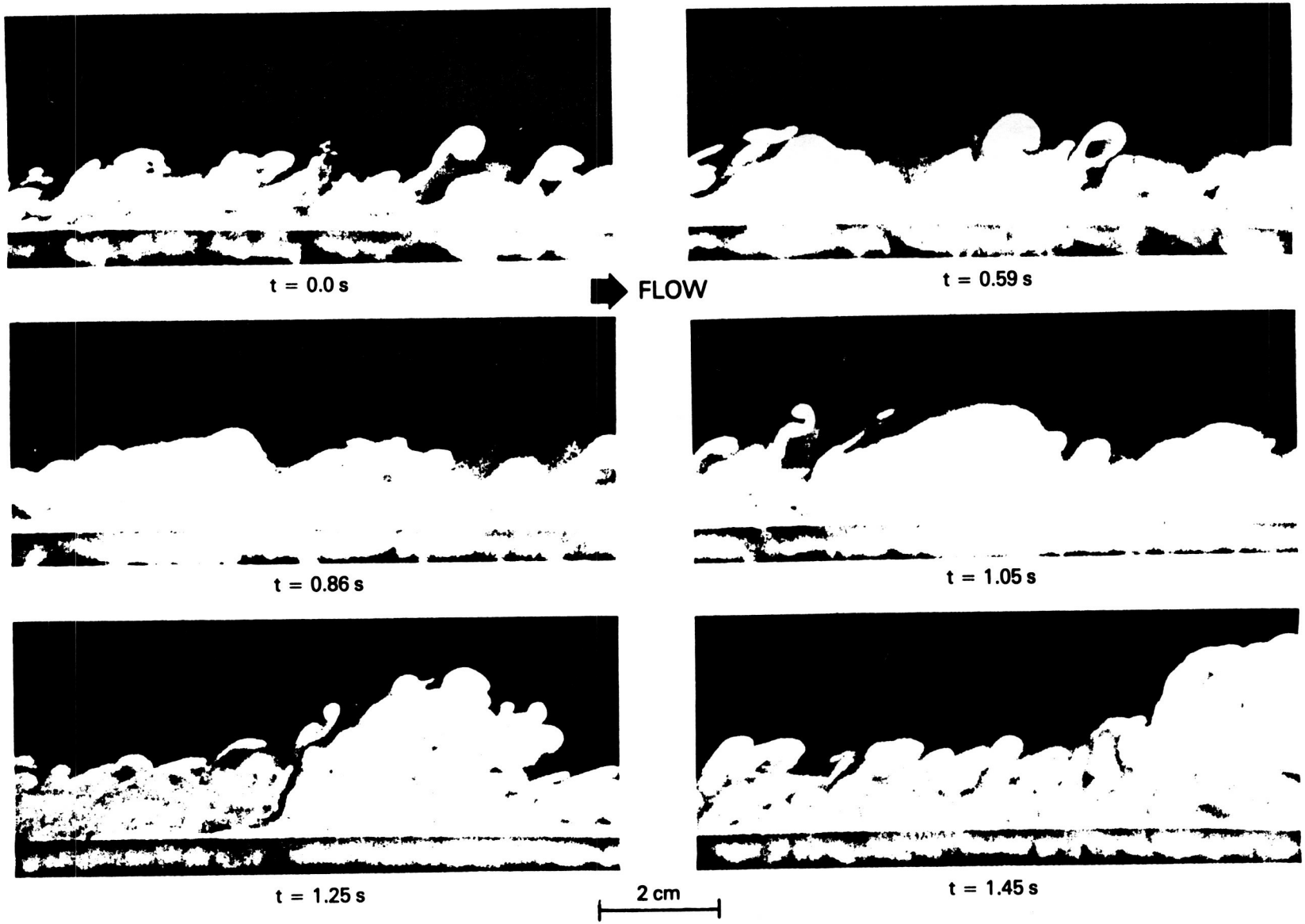

Figure 12. **Turbulent Boundary Layer is Marked by Dark Yellow Dye. A Lighter Dye Marks the Periodic Flow from the Spanwise Slot. Although the Initial Spanwise Vortex Introduced into the Boundary Layer is Relatively Small, its Interaction with the Natural Eddies Results in a Very Large Bulge**

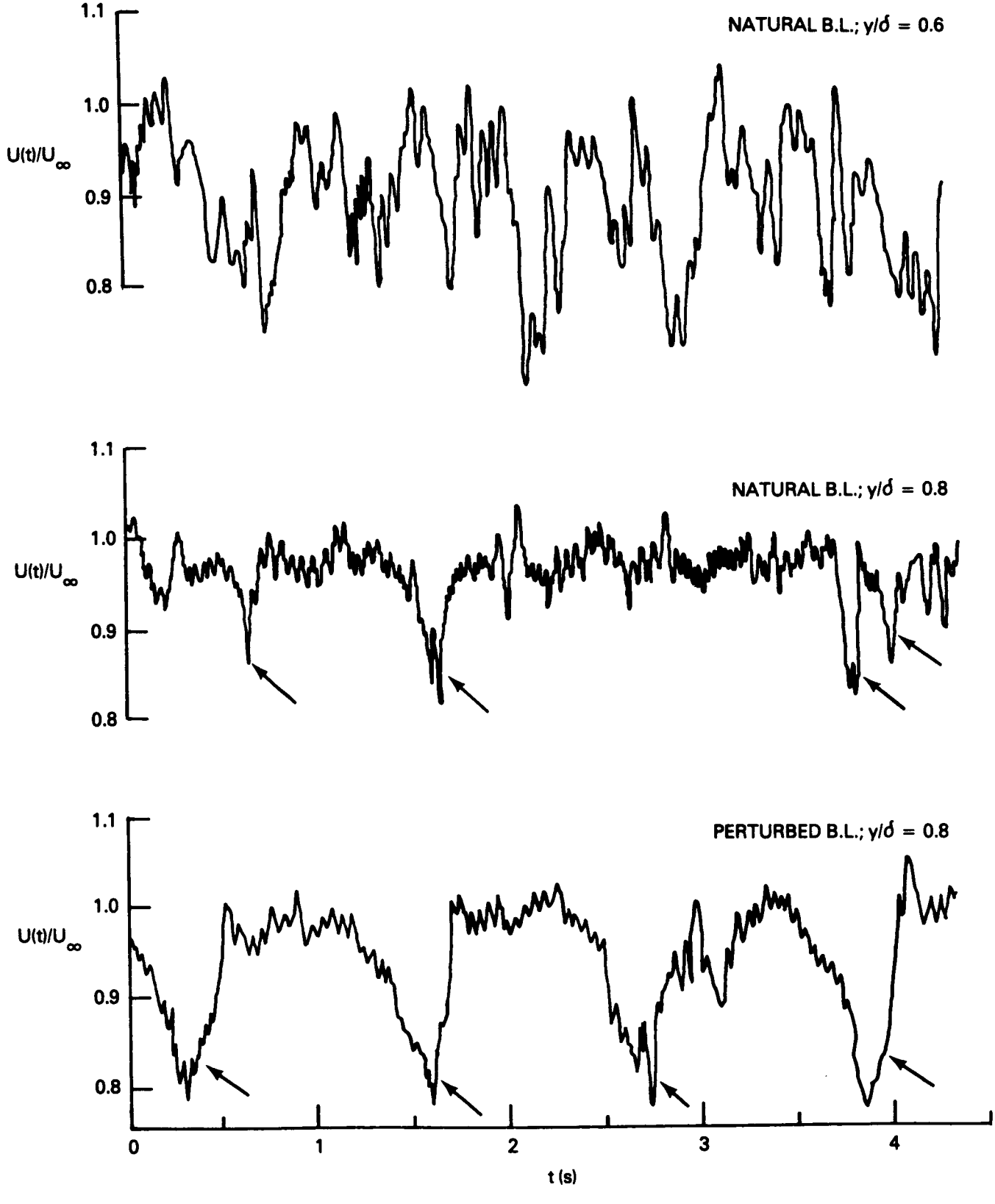

Figure 13. Instantaneous Streamwise Velocity Records. U_∞ = 20 cm/s; x = 100 cm

fixed probe are still perfectly periodic. Some differences exist, however, between the velocity signature of the natural eddies and the artificial ones. Although this does not seem to be important for the particular application sought by the present investigation, the injection parameters can further be optimized to produce the desired spike's configuration.

The repeatability of the artificial structures is evident from the instantaneous streamwise velocity record depicted in Figure 14. The maximum injection speed in this run is twice the ambient flow speed. The mean speed recorded by the probe at this position is 18.48 cm/s, slightly lower than that recorded at the same position in the absence of cyclic perturbations (19.21 cm/s). The negative spikes shown in Figure 14 are perfectly periodic but some slight changes in their amplitude are observed and are probably caused by their interactions with the random background turbulence. It is also interesting to note that, when the boundary layer is perturbed, the artificially generated periodic structures dominate the flow and the naturally occurring random eddies are no longer observed visually or with a hot-film probe. Apparently the periodic excitations interact with whatever mechanism (bursting, entrainment, etc.) generating the large-eddy structures in the first place to produce periodic eddies.

In summary, cyclic injection from a spanwise slot generates periodic structures that appear visually to resemble the random, naturally occurring large eddies. The velocity signature of the artificial structures is also similar to the natural large-eddy structures. The artificially generated periodic structures dominate the flow and the naturally occurring random eddies are no longer observed.

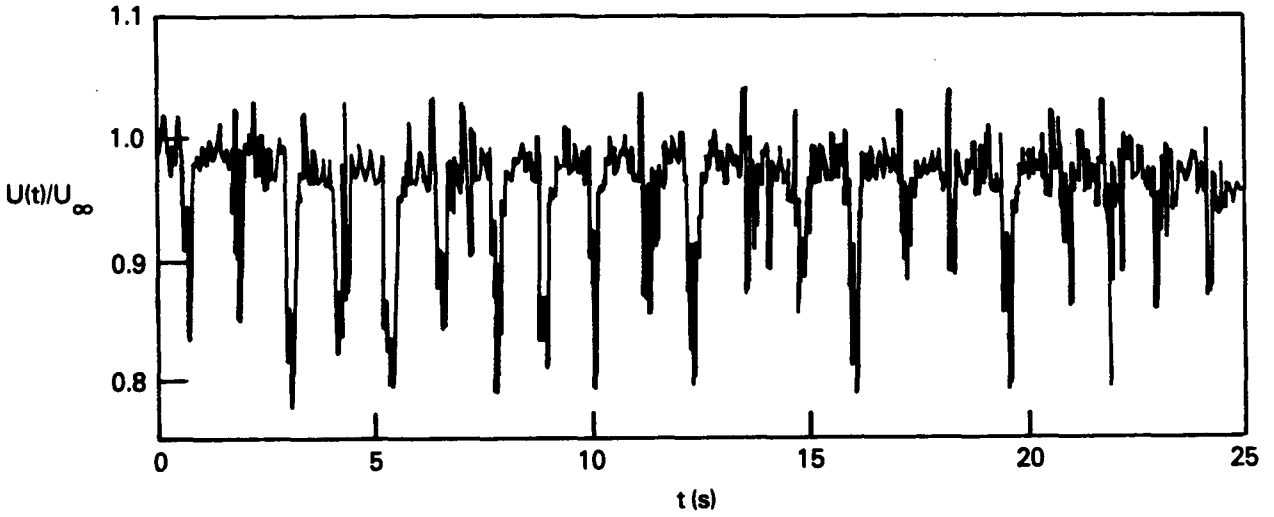

Figure 14. **Instantaneous Streamwise Velocity Records. Twenty One Large Eddy Structures were Artificially Generated from the Spanwise Injection Slot. U_∞ = 20 cm/s; x = 100 cm; y/δ = 0.8; Maximum Injection Speed = 40 cm/s**

6. EFFECTS OF ARTIFICIAL LARGE-SCALE STRUCTURES ON BURSTING

The purpose of the device considered in the present study is to produce periodic structures that are similar to the random, naturally occurring, large-eddy structures. Together with adaptive optics, such device may be used on airborne laser platforms to reduce or eliminate optical distortion caused by the turbulence in the aircraft's boundary layer. In Section 5, the similarity between the artificial (periodic) structures and the natural (random) ones has been established. An unexpected additional benefit of the large-eddy generating device was discovered during the present experiments. It seems that the periodic large-eddy structures trigger the generation of bursting events near the wall of the flat plate. That is, not only the large eddies that characterize the outer parts of a turbulent boundary layer become periodic, but also the near-wall bursts, which randomly occur in a natural boundary layer, seem to be occurring periodically. The present section establishes this result. We start with a brief recap of the bursting phenomenon.

The wall region of a turbulent boundary layer is dominated by a sequence of intense organized motions that are collectively called the bursting phenomenon (Kline et al., 1967). According to at least one school of thought, the process begins with a pair of elongated, steamwise, counter-rotating vortices. These vortices exist in a strong shear and induce low- and high-speed regions between them. Both the vortices and the accompanying eddy structures occur randomly in space and time. The low-speed regions appear to grow downstream, lift up and develop inflectional velocity profiles. At approximately the same time, the interface between the low- and high-speed fluid begins to oscillate. The low-speed region lifts up away from the wall as the oscillation amplitude increases, resulting in chaotic breakdown of the streak. Since this latter process occurs on a very short time scale, Kline (1978) called it a 'burst'.

A side view of a naturally occurring bursting event is shown in Figure 15. The freestream speed is 20 cm/s and the wall region at x = 100 cm is visualized using fluorescent dye seeping from a spanwise slot just upstream of the observation station. The dye is excited with a vertical sheet of laser light parallel to the flow direction, and the flow is from left to right. The time measured from an arbitrary origin is indicated underneath each photograph. The apparent accumulation of dye is caused by the formation of a low-speed region, and the lifting and breakup of this region is evident in the photographic sequence shown in the figure.

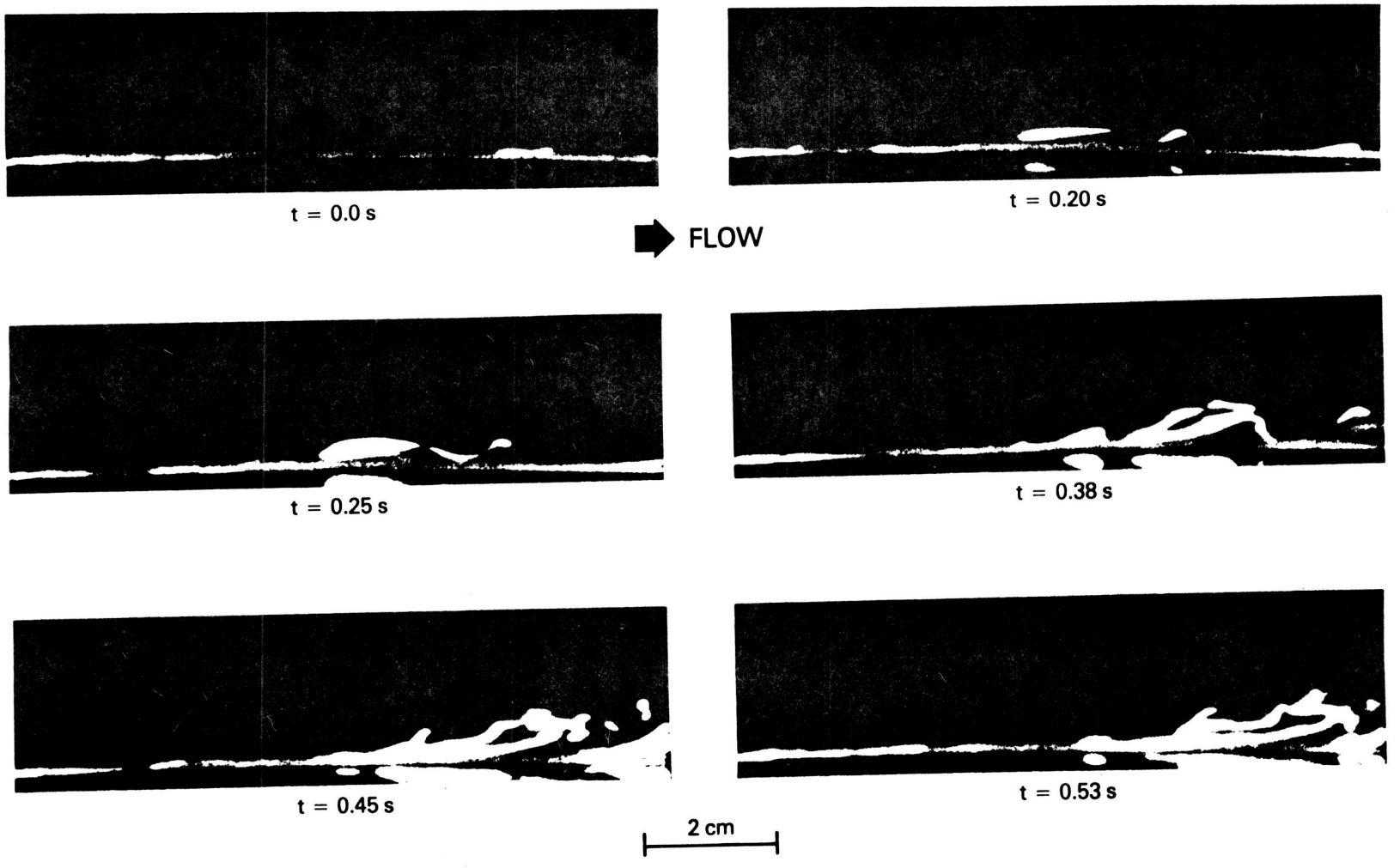

Figure 15. Naturally Occurring Bursting Events in a Turbulent Boundary Layer

As shown by Gad-el-Hak & Hussain (1986), bursting events can also be induced artificially by withdrawing near-wall fluid from two minute holes separated in the spanwise direction or by pitching a miniature delta wing that is flush-mounted to the wall. Either of these two actions generates a hairpin-like vortex and low-speed streak that resemble naturally occurring structures. The resulting sequence of events that occur at a given location can then be uniquely controlled, thus allowing detailed examination via phase-locked measurements.

In contrast to the above method of inducing bursts by simulating wall events, in the present investigation the passing of an artificially induced, periodic large-eddy structure seems to trigger a bursting event near the wall. This is shown convincingly in the visualization results depicted in Figures 16 and 17. In both figures, the flow is from left to right, the freestream speed is 20 cm/s, and the observation station is 100 cm downstream of the leading edge. For the case depicted in Figure 16, the maximum injection speed is 45 cm/s, the ball valve's duty cycle is symmetric with opening time = closing time = 0.1 s. A slow closing (closing time = 1 s), fast opening (0.1 s) and lower maximum injection speed (20 cm/s) are the parameters of the run shown in Figure 17. In both cases, it is evident that the passing of the artificially generated large-eddy structure triggers a burst-like event in the wall region. As shown in the ciné films from which these selected still photographs were taken, the bursting event was periodic, having exactly the same frequency as the structure that induced it.

The pattern-recognition algorithms described in Section 3.6 were used to establish the similarity between the artificially induced wall events and the naturally occurring ones. The streak detector searches for low-speed regions near the wall relative to the background mean velocity. The burst detector searches for periods of high acceleration without necessarily larger fluctuations than the background turbulence. As shown by Blackwelder & Kaplan (1976), such periods are associated with events characterized by a high degree of coherence in time and in the direction normal to the wall and having a conditionally-averaged Reynolds shear stress that is an order of magnitude greater than its conventionally-averaged value. The detection scheme is then based on the kinematics and indirectly on the dynamic properties of the organized structure.

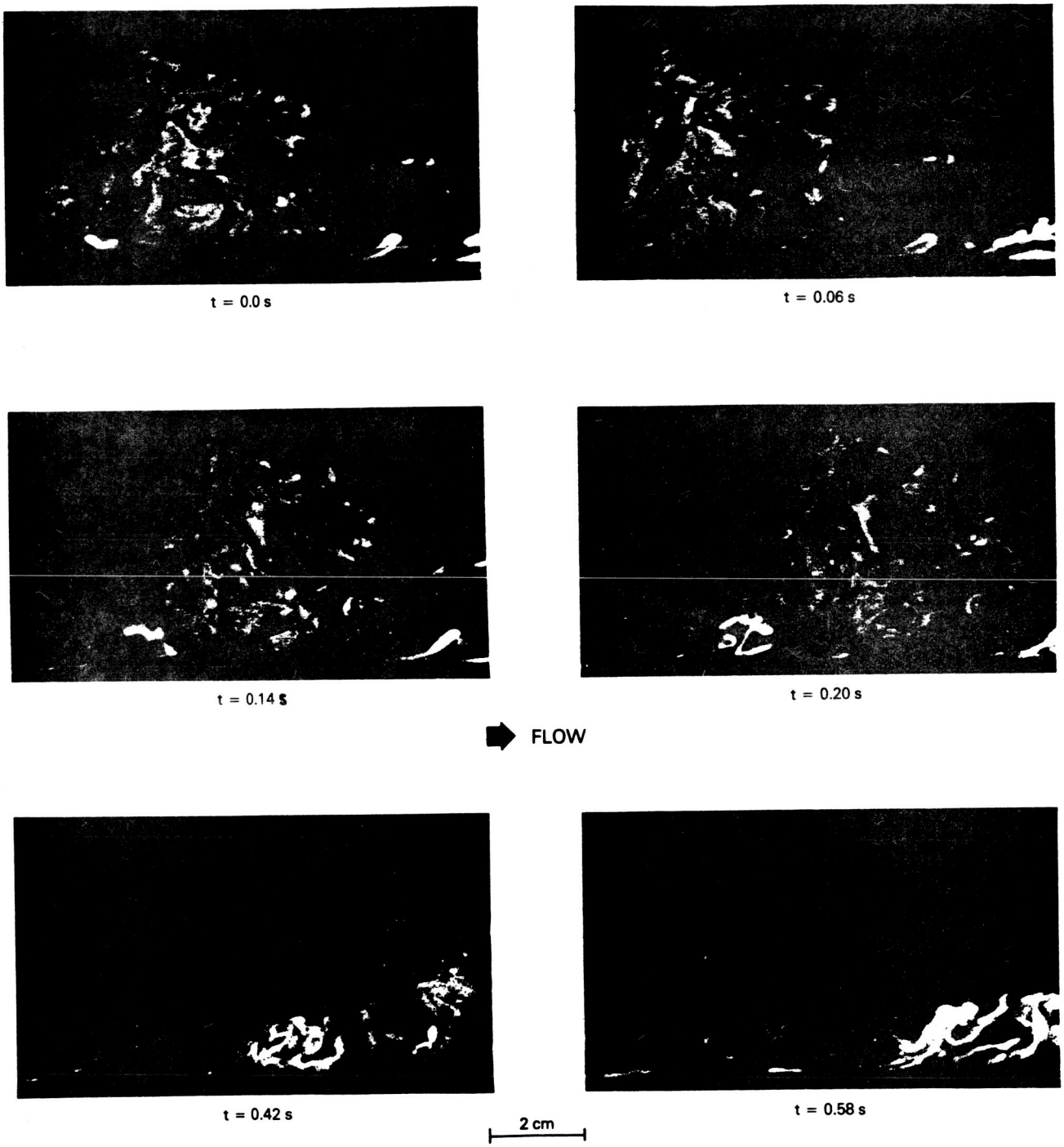

Figure 16. A Bursting Event Triggered by the Passing of an Artificial Large Eddy Structure

Figure 17. A Bursting Event Triggered by the Passing of an Artificial Large Eddy Structure

Whenever an artificially generated large-eddy structure passed on top of the velocity probe located very near the wall, a low-speed streak and a burst were detected by the two pattern-recognition algorithms; thus further confirming the visualization results depicted in Figures 16 and 17.

In summary, the cyclic injection from a spanwise slot seems to generate periodic structures similar to the random, naturally-occurring large eddies. These structures in turn appear to trigger periodic bursting events near the wall, even at stations far downstream of the large-eddy generating device. Thus, the present device generates periodic structures in both the outer and inner regions of a turbulent boundary layer. The degree of two dimensionality of the artificial large-eddy structures and the spanwise periodicity of the bursting events are important issues that have not been investigated in the present preliminary study.

7. SPECTRAL ANALYSIS

The autocorrelation and spectrum of the longitudinal velocity fluctuations are two statistical quantities useful in analyzing the intermittent signal from a hot-film probe located near the outer portion of a turbulent boundary layer and the effects of the large-eddy generating device. At a given spatial location, the autocorrelation coefficient is the correlation between the values of the streamwise velocity fluctuations, u, at two different times nondimensionalized using the mean square:

$$R(\tau) = \frac{\overline{u(t)\ u(t-\tau)}}{\overline{u^2}} \quad ,$$

where the overbar denotes a time average. The Fourier transform of the autocorrelation coefficient is the power spectral density:

$$S(f) = \frac{1}{2\pi} \int_{-\infty}^{\infty} e^{-2\pi\tau f}\ R(\tau)\ d\tau \quad ,$$

which is the normalized spectral distribution of the squared intensity of the longitudinal velocity fluctuations (Hinze, 1975). These two functions provide a convenient method of determining length scales in the flow field and may provide clues to periodic and/or other structures embedded in the random velocity fluctuations.

The effects of the large-eddy generating device on the dimensional spectral distribution [$S'(f) = \overline{u^2}S(f)$] and the autocorrelation coefficient are eluciated by comparing these statistical quantities for a natural boundary layer (Figure 18) and a perturbed one (Figure 19). In both cases, the freestream speed is 20 cm/s and the probe is located at x = 67 cm and $y/\delta = 0.6$. For the perturbed case shown in Figure 19, the maximum injection speed is 40 cm/s and the cyclic jet is on for 0.1 s and off for 0.4 s. A pronounced spectral peak is evident in Figure 19 at a frequency of 2 Hz. Also, a corresponding oscillation appears in the correlation coefficient with a period of 0.5 s, exactly equal to the period of the cyclic jet.

Similar comparison is made further downstream at x = 100 cm and $y/\delta = 0.8$, and this is shown in Figures 20 and 21 for the natural case and the perturbed case, respectively. The maximum injection speed for the perturbed case is

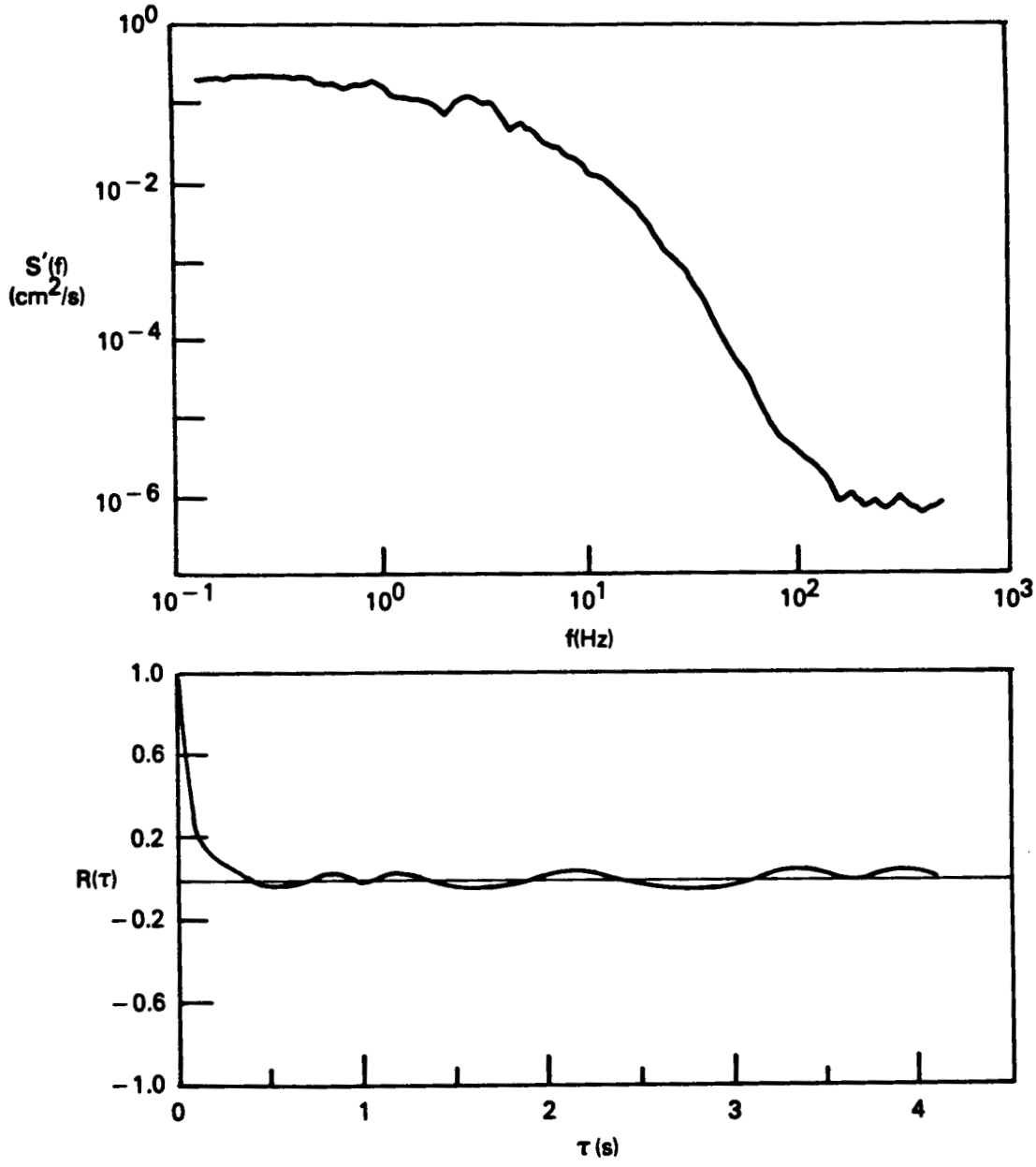

Figure 18. Spectrum and Autocorrelation for Natural Boundary Layer. U_∞ = 20 cm/s; x = 67 cm; y/δ = 0.6

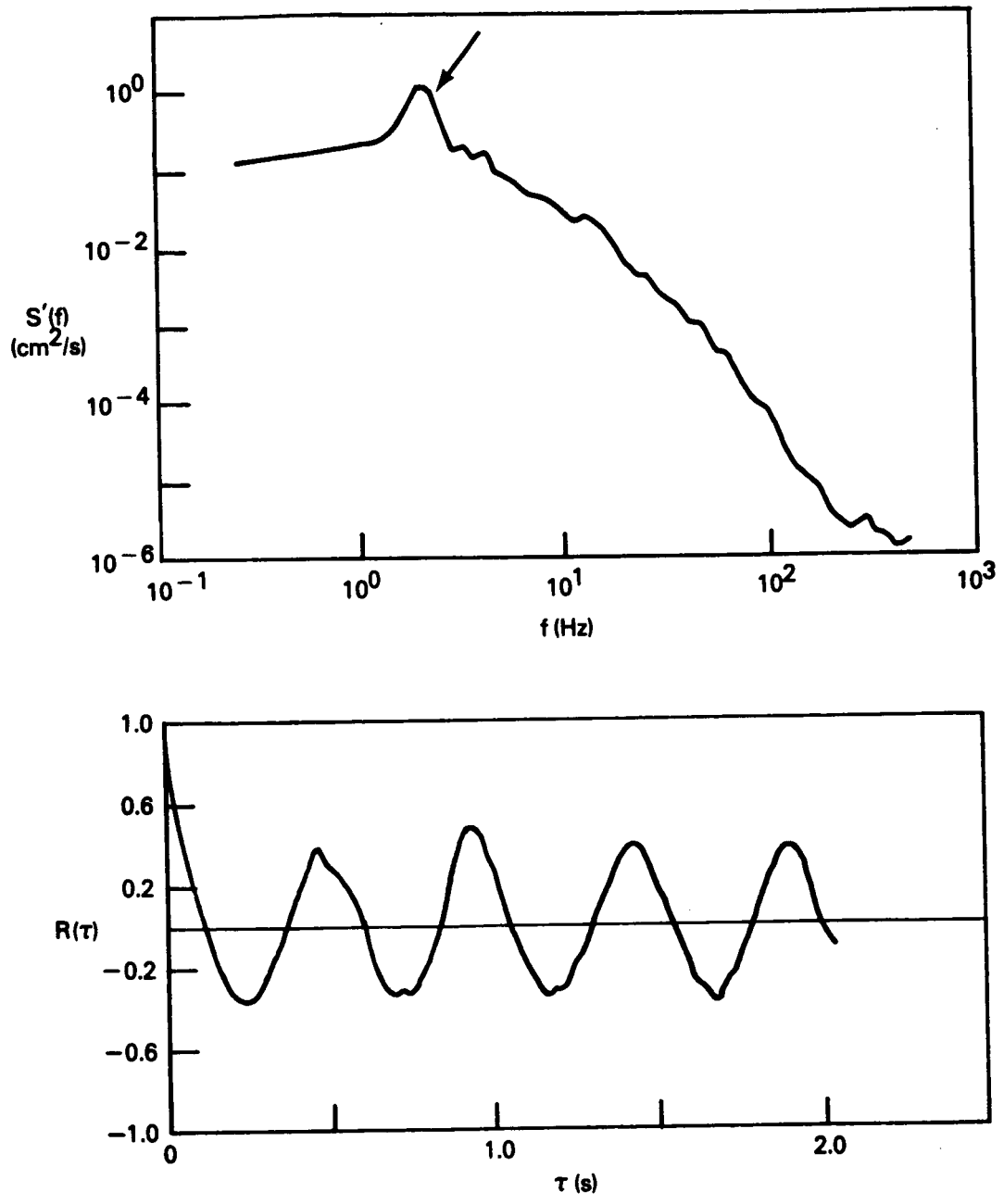

Figure 19. Spectrum and Autocorrelation for Perturbed Boundary Layer. U_∞ = 20 cm/s; x = 67 cm; y/δ = 0.6; Maximum Injection Speed = 40 cm/s

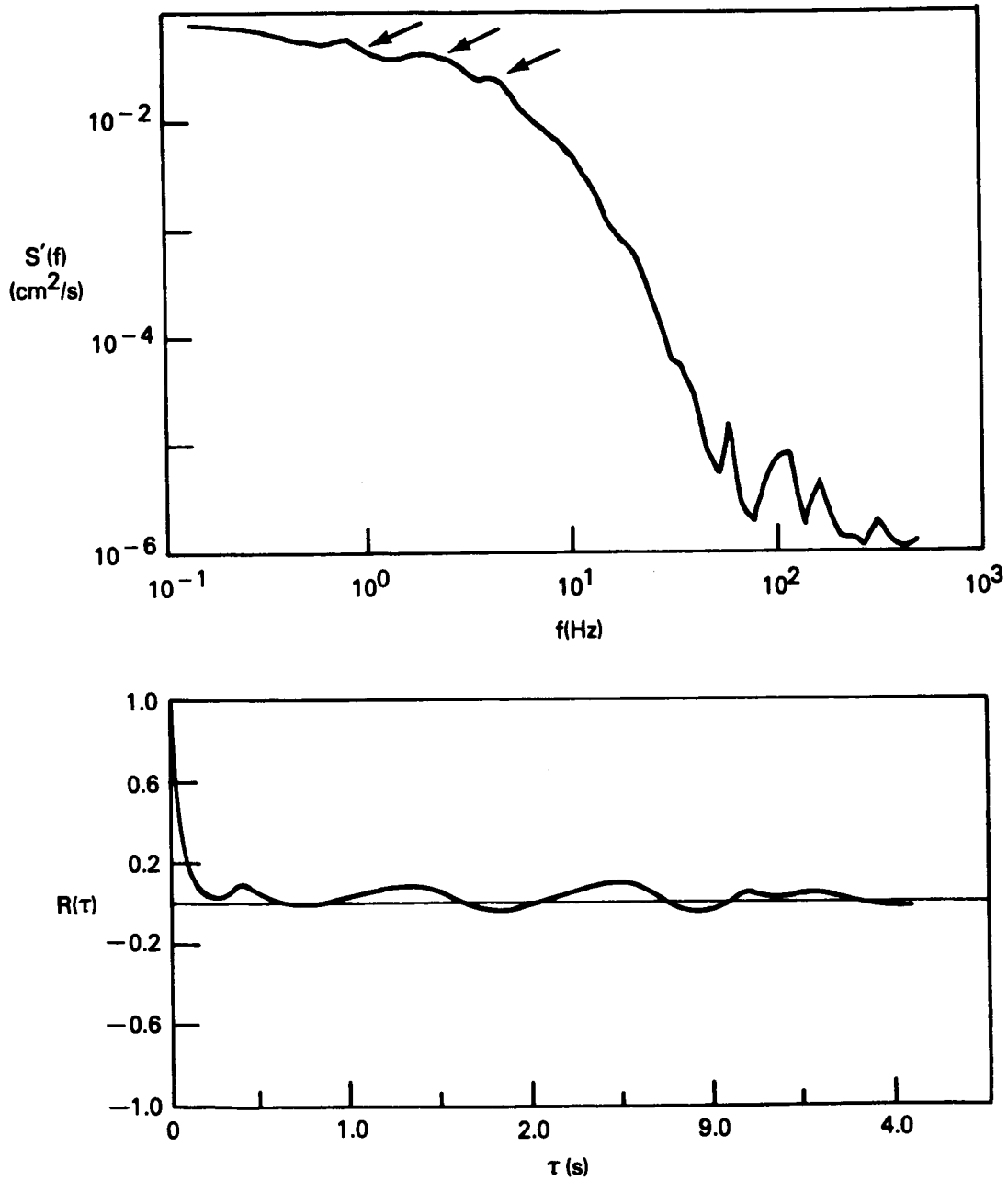

Figure 20. Spectrum and Autocorreltion for Natural Boundary Layer. U_∞ = 20 cm/sec; x = 100 cm; y/δ = 0.8

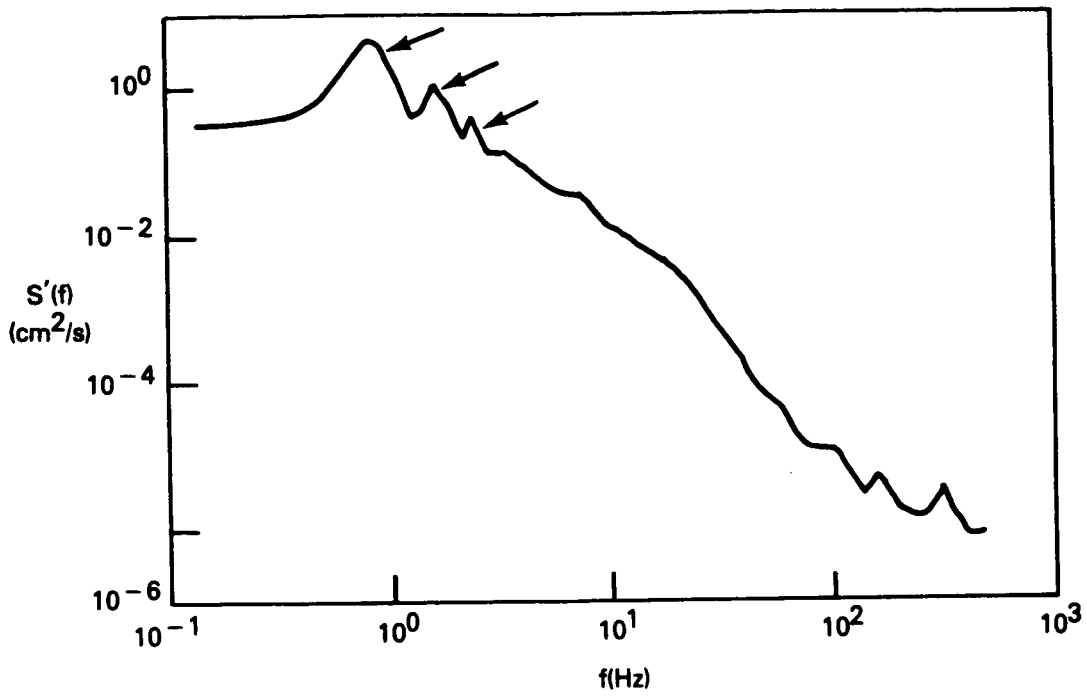

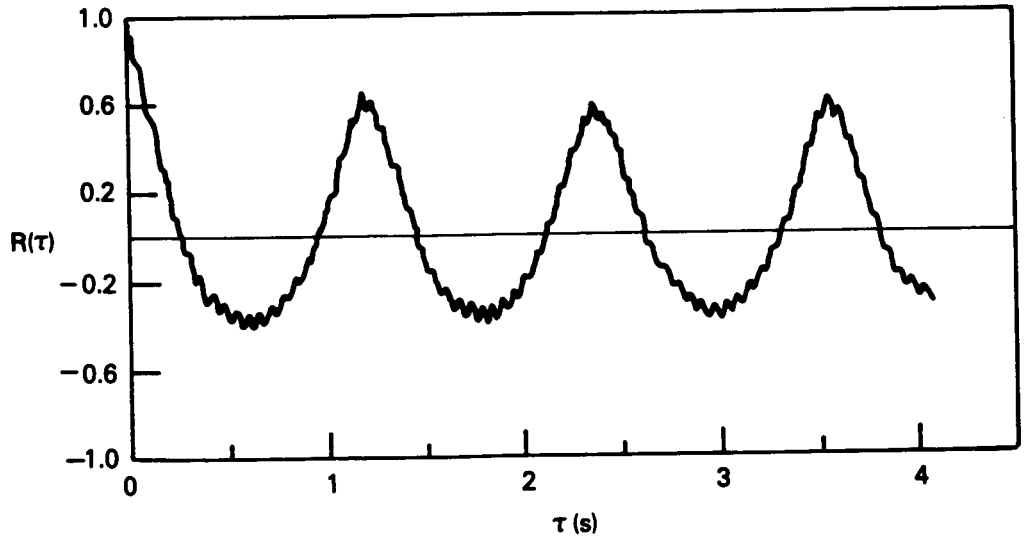

Figure 21. Spectrum and Autocorrelation for Perturbed Boundary Layer. U_∞ = 20 cm/s; x = 100 cm; y/δ = 0.8; Maximum Injection Speed = 40 cm/s

unchanged (40 cm/s), but the ball valve opens more slowly in this latter comparison (opening time = 1 s; closing time = 0.25 s). A slight peak appears in the spectrum of the natural boundary layer (Figure 20). At this higher position, the mean frequency of the natural large-eddy structures is 0.9 Hz. Two other peaks are observed in the same figure, corresponding to the first and second harmonics. In the perturbed case, all three peaks are much more pronounced and a well-defined period of 1.25 s is observed in the autocorrelation coefficient. It is interesting to note that the oscillations in the autocorrelation coefficient are symmetric in the case of fast opening and slow closing ball valve (Figure 19) and quite asymmetric when the ball valve opens slowly and close fast (Figure 21).

As evident from comparing the area under the spectral distribution curves for the natural and perturbed boundary layers, the mean square of the steamwise velocity fluctuations is increased by the introduction of the cyclic secondary fluid into the turbulent boundary layer. This means that an increase in the turbulence level is a penalty associated with making the large-eddy structures periodic. More work is needed to investigate this point, specially whether or not further optimization of the device will lead to better management of the level of turbulence.

8. PROBABILITY DISTRIBUTION

A useful statistical quantity that may shed some light on the effects of the large-eddy generating device on the flow field is the probability density function of the steamwise velocity fluctuations (Lumley, 1970; Tennekes & Lumley, 1972). In Figure 22, comparison is made between the probability density function for the natural boundary layer and the perturbed one. The abscissa in the figure is the streamwise velocity, and the ordinate is a normalized probability density function such that the area under the curve is unity. For both cases depicted in the figure, the freestream speed is 20 cm/s and the hot-film probe is located at $x = 67$ cm (5 cm downstream of the spanwise injection slot) and $y/\delta = 0.6$. The maximum injection speed is 40 cm/s and the duty cycle of the ball valve consists of fast opening (0.1 s) followed by slow closing (0.4 s). Both probability distributions are slightly skewed, i.e., the mean velocity is slightly lower than the most probable velocity. The distribution in the perturbed case is more broad, however, consistent with the higher turbulence levels.

The negative skewness of the perturbed case is more pronounced in the case shown in Figure 23. In here $x = 100$ cm, $y/\delta = 0.6$, and the duty cycle of the ball valve consists of slow opening (1 s) followed by fast closing (0.25 s). At higher probe position, $y/\delta = 0.8$, the turbulence level is lower and the probability distribution is narrower, as shown in Figure 24. All the other run parameters in both the natural and perturbed cases are the same as those for the runs depicted in Figure 23.

In summary, it appears that the large-eddy generating device results in a broader, more negatively skewed probability distribution. Both these effects are a result of the higher turbulence levels generated by the cyclical injection and are consistent with the instantaneous velocity records depicted in Figures 13 and 14.

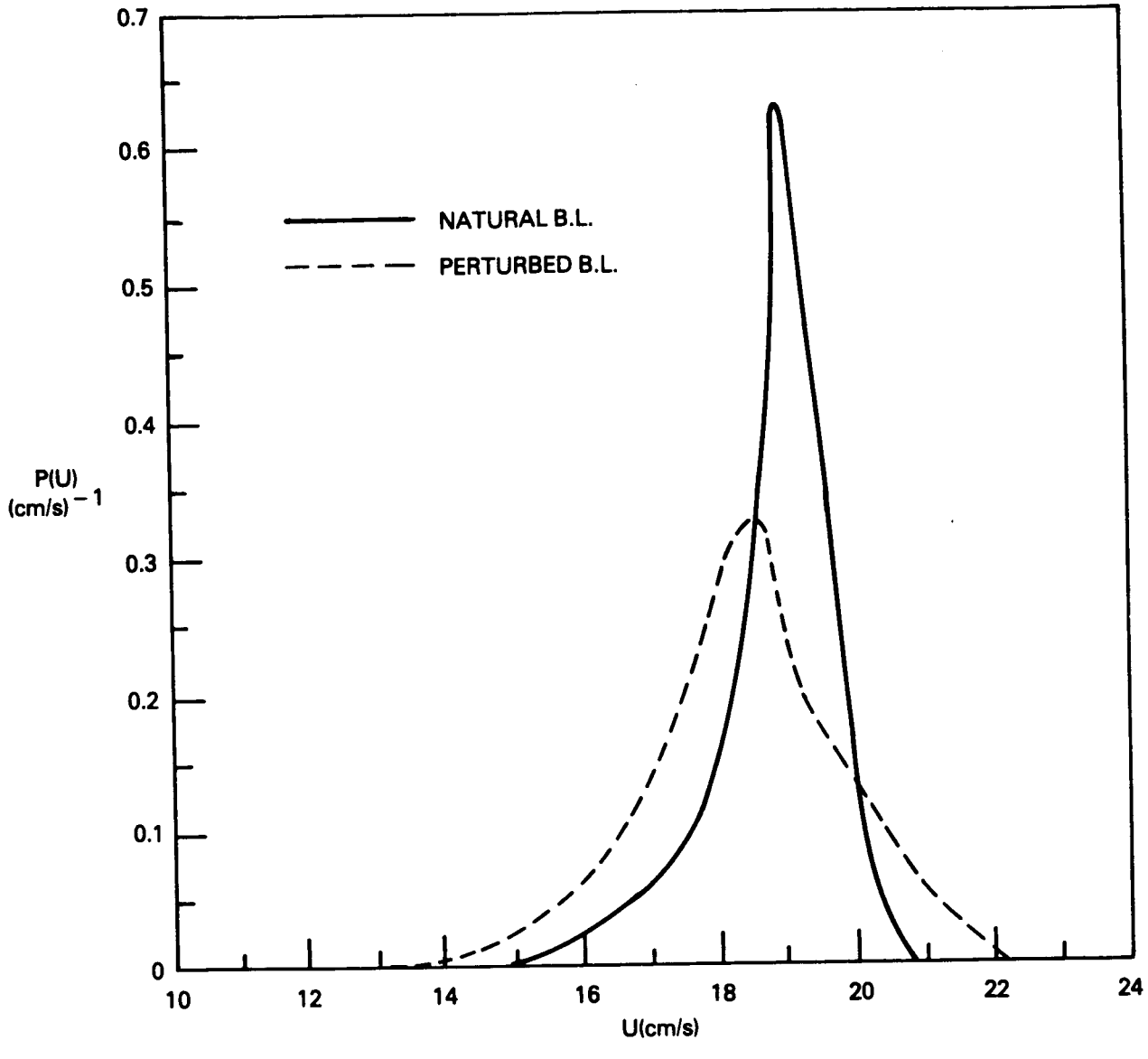

Figure 22. Effects of Periodic Injection on Probability Density Function. U_∞ = 20 cm/s; x = 67 cm; y/δ = 0.6

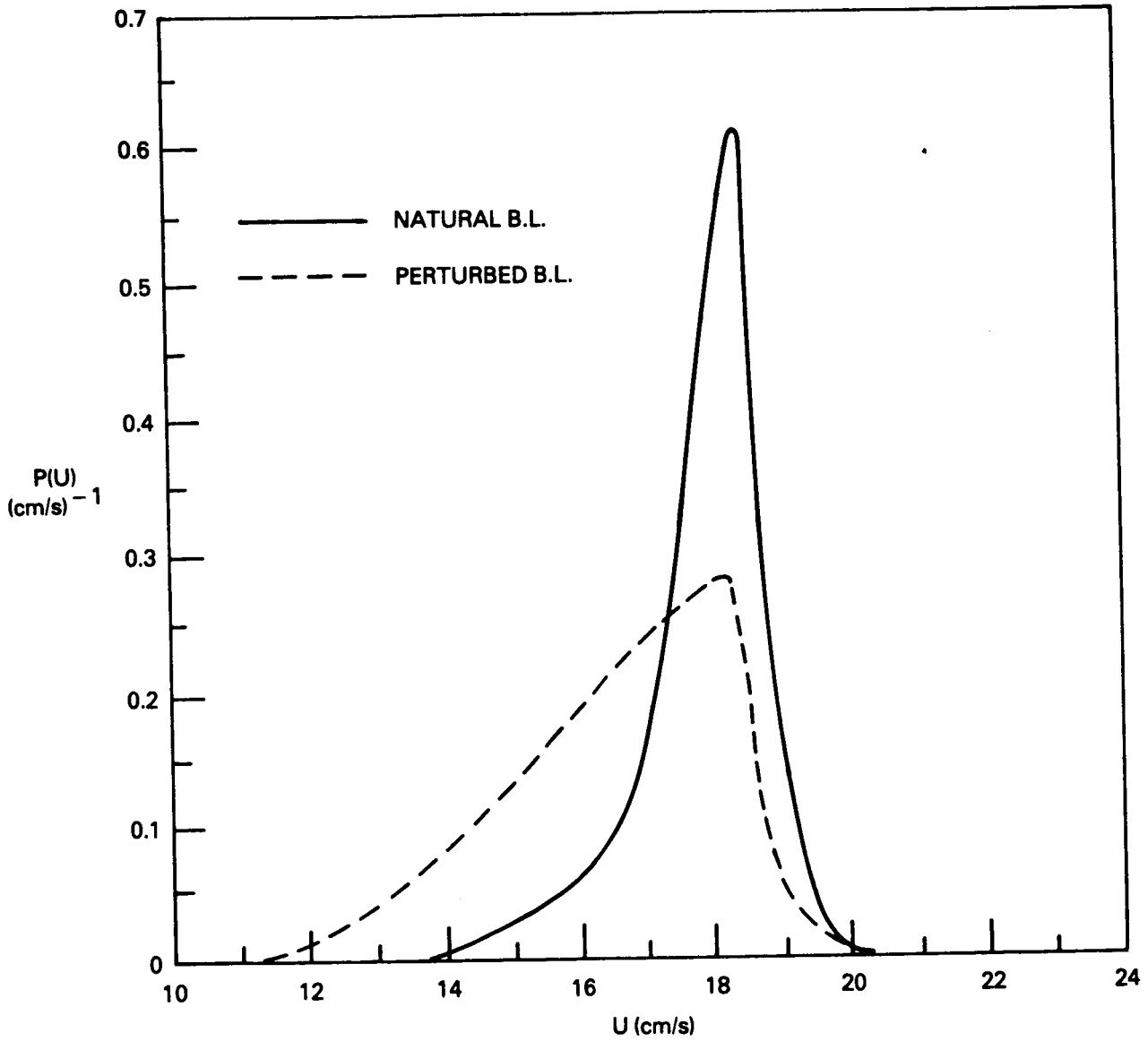

Figure 23. Effects of Periodic Injection on Probability Density Function U_∞ = 20 cm/s; x = 100 cm; y/δ = 0.6

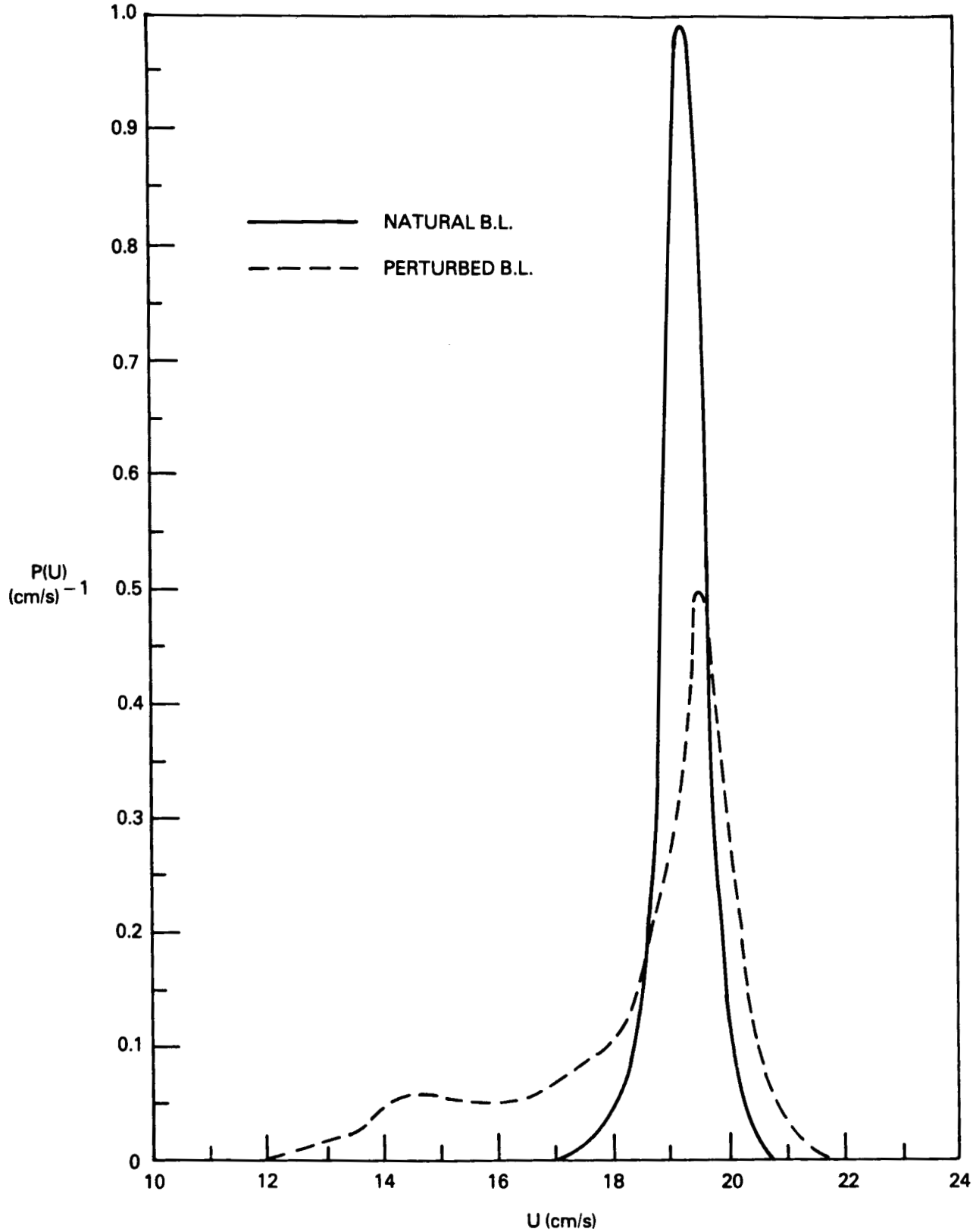

Figure 24. Effects of Periodic Injection on Probability Density Function. U_∞ = 20 cm/s; x = 100 cm; y/δ = 0.8

9. SUMMARY

An active flow control device to generate large-scale, periodic structures in a turbulent boundary layer was considered in the present experimental investigation. Together with adaptive optics, the device may be used on airborne laser platforms to reduce or eliminate optical distortion caused by the turbulence in the aircraft's boundary layer. Periodic large-eddy structures were artificially generated by cyclically injecting secondary fluid from a spanwise slot. A flat plate towed in a water channel was used as a test bed to establish the feasibility of the flow control device. The boundary layer flow was visualized using either hydrogen bubbles shed from a stainless-steel wire or fluorescent dyes injected either from the large-eddy generating device or from a second, downstream spanwise slot. Both the hydrogen bubbles and the fluorescent dyes were illuminated using sheets of laser light projected in the desired plane. Hot-film probes were used to record the longitudinal velocity fluctuations. Important statistical quantities, such as the mean, the root-mean-square, the autocorrelation, the spectrum, and the probability distribution were computed from the instantaneous velocity records to assess the effectiveness of the flow control device.

A high degree of control of the cyclical injection was achieved by using a pressure regulator and a computer driven ball valve. Within the limitations of the experimental apparatus, the maximum injection speed from the spanwise slot, the acceleration and deceleration rates of secondary fluid's injection, and the delay time between successive cycles can be changed to optimize the simulation of large-eddy structures in a given turbulent boundary layer.

The periodic structures generated from the spanwise injection device were shown to be similar to the random, naturally occurring, large-eddy structures. The negative spikes resulting from the passing of the artificial eddies by a fixed hot-film probe were still perfectly periodic at a distance 12δ downstream of the large-eddy generating device. Some differences existed, however, between the velocity signature of the natural eddies and the artificial ones. Although this may not be important for the particular application sought by the present research, the injection parameters can further be optimized to produce the desired spike's configuration. The artificially generated periodic structures dominate the flow, and the natural random eddies are no longer

observed visually or with a hot-film probe. Apparently the periodic excitations interact with whatever mechanism generating the random large eddies in the first place to produce periodic eddies.

At a given location in the boundary layer, the injection device resulted in slightly lower mean velocity but higher turbulence levels. A dominant spectral peak and a corresponding oscillation in the autocorrelation coefficient appeared at the injection frequency. Two other peaks in the spectral distribution corresponded to the first and second harmonics of the perturbation frequency. The probability distributions were more broad and more negatively skewed in the case of the perturbed boundary layer as compared to the distributions in a natural turbulent boundary layer.

In addition to removing the inherent randomness in large-eddy structures, the periodic large eddies generated from the spanwise slot seemed to trigger the generation of bursting events near the wall of the flat plate. Thus, both the large eddies and bursts occurred periodically in the perturbed turbulent boundary layer, even at stations far downstream of the large-eddy generating device. In other words, the device considered in the present investigation is capable of producing periodic structures in both the outer and inner regions of a turbulent boundary layer. There are, however, some important issues that remain to be addressed by future research. For example, the degree of two dimensionality of the artificial structures, the spanwise periodicity of the bursting events, and methods to reduce the high turbulence levels introduced by the control device. Future research will also be conducted to investigate the control of a free shear layer using subharmonic perturbations, as was briefly discussed in Section 2.

REFERENCES

Blackwelder, R. F., and Kaplan, R. E. (1976) "On the Wall Structure of the Turbulent Boundary Layer," J. Fluid Mech. 76, p. 89.

Brown, G. L., and Roshko, A. (1971) "The Effect of Density Differences on the Turbulent Mixing Layer," Turbulent Shear Flows, AGARD CP-93, p. 23-1.

Brown, G. L., and Roshko, A. (1974) "On Density Effects and Large Structure in Turbulent Mixing Layers," J. Fluid Mech. 64, p. 775.

Bushnell, D. (1983) "Turbulent Drag Reduction for External Flows," AIAA Paper No. 83-0227.

Chernov, L. A. (1967) Wave Propagation in a Random Medium, Dover, New York.

Christiansen, W. H., Russell, D. A., and Hertzberg, A. (1975) "Flow Lasers," Ann. Rev. Fluid Mech. 7, p. 115.

Corke, T. C. (1981) "A New View on Origin, Role and Manipulation of Large Scales in Turbulent Boundary Layers," Ph.D. Thesis, Illinois Institute of Technology, Chicago.

de Jonckheere, R. K., and Chou, D. C. (1982) "Experimental and Analytical Scaling on the Flowfield Around a Protuberance at High Subsonic Speed," AIAA Paper No. 82-1371.

de Jonckheere, R. K., and Chou, D. C. (1983) "Active Flow Control Effects on Boundary Layer Development Around a Protuberance at High Subsonic Speed," AIAA Paper No. 83-1737.

de Jonckheere, R. K., Russell, J. J., and Chou, D. C. (1982) "High Subsonic Flowfield Measurements and Turbulent Flow Analysis Around a Turret Protuberance," AIAA Paper No. 82-0057.

Gad-el-Hak, M. (1986a) "The Use of the Dye-Layer Technique for Unsteady Flow Visualization," J. Fluid Engineering 108, p. 34.

Gad-el-Hak, M. (1986b) "Review of Flow Visualization Techniques for Unsteady Flows," Exp. Fluids, in press.

Gad-el-Hak, M. (1986c) "The Water Towing Tank as an Experimental Facility," Exp. Fluids, in press.

Gad-el-Hak, M., and Blackwelder, R. F. (1985) "The Discrete Vortices from a Delta Wing," AIAA Journal 23, p. 961.

Gad-el-Hak, M., and Blackwelder, R. F. (1986a) "Control of the Discrete Vortices from a Delta Wing," AIAA Paper No. 86-1915.

Gad-el-Hak, M., and Blackwelder, R. F. (1986b) "Control of the Discrete Vortices from a Delta Wing," submitted to AIAA J.

Gad-el-Hak, M., Blackwelder, R. F., and Riley, J. J. (1981) "On the Growth of Turbulent Regions in Laminar Boundary Layers," J. Fluid Mech. 110, p. 73.

Gad-el-Hak, M., Blackwelder, R. F., and Riley, J. J. (1984) "On the Interaction of Compliant Coatings with Boundary Layer Flows," J. Fluid Mech. 140, p. 257.

Gad-el-Hak, M., and Hussain, A. K. M. F. (1986) "Coherent Structures in a Turbulent Boundary Layer. Part 1: Generation of 'Artificial' Bursts," Phys. Fluids 29, p. 2124.

Hinze, J. O. (1975) Turbulence, Second Edition, McGraw-Hill, New York.

Ho, C.-M., and Huang, L.-S. (1982) "Subharmonic and Vortex Merging in Mixing Layers," J. Fluid Mech. 119, p. 443.

Ho, C.-M., and Huerre, P. (1984) "Perturbed Free Shear Layers," Ann. Rev. Fluid Mech. 16, p. 365.

Kline, S. J. (1978) "The Role of Visualization in the Study of the Structure of the Turbulent Boundary Layer," in Coherent Structure of Turbulent Boundary Layers, eds. C. R. Smith & D. E. Abbott, Lehigh University, Bethlehem, PA, p. 1.

Kline, S. J., Reynolds, W. C., Shraub, F. A., and Runstadler, P. W. (1967) "The Structure of Turbulent Boundary Layers," J. Fluid Mech. 30, p. 741.

Kovasznay, L. S. G., Kibens, V., and Blackwelder, R. F. (1970) "Large-Scale Motion in the Intermittent Region of a Turbulent Boundary Layer," J. Fluid Mech. 41, p 283.

Lumley, J. L. (1970) Stochastic Tools in Turbulence, Academic Press, New York.

Oster, D., Wygnanski, I., Dziomba, B., and Fiedler, H. (1978) "On the Effect of Initial Condition on a Two-Dimensional Mixing Layer," Lecture Notes in Physics 75, Springer, Berlin, p. 48.

Purtell, L. P., Klebanoof, P. S., and Buckley, F. T. (1981) "Turbulent Boundary Layer at Low Reynolds Number," Phys. Fluids 24, p. 802.

Russell, D. A. (1974) "Fluid Mechanics of High Power Grid Nozzle Lasers," AIAA Paper No. 74-223.

Smith, F. L., Chou, D. C., and de Jonckheere, R. K. (1985) "Passive Control Effects on Flow Separation Around a Proturberance at High Subsonic Speed," AIAA Paper No. 85-0351.

Tennekes, H., and Lumley, J. L. (1972) A First Course in Turbulence, MIT Press, Cambridge, MA.

Viets, H. (1980) "Coherent Structures in Time Dependent Shear Flows," Turbulent Boundary Layers, AGARD CP-271, p. 5-1.

Viets, H., Ball, M., and Bougine, D. (1981) "Performance of Forced Unsteady Diffusers," AIAA Paper No. 81-0154.

Winant, C. D., and Browand, F. K. (1974) "Vortex Pairing: The Mechanism of Turbulent Mixing-Layer Growth at Moderate Reynolds Number," J. Fluid Mech. 63, p. 237.

Standard Bibliographic Page

1. Report No.	2. Government Accession No.	3. Recipient's Catalog No.
NASA CR-178249		

4. Title and Subtitle	5. Report Date
Turbulence Control on an Airborne Laser Platform	March 1987
	6. Performing Organization Code
7. Author(s)	8. Performing Organization Report No.
Mohamed Gad-el-Hak	Flow Res. Rept. No. 365
9. Performing Organization Name and Address	10. Work Unit No.
Flow Research Company/Flow Industries, Inc. 21414 68th Avenue S. Kent, WA 98032	11. Contract or Grant No. NAS1-18213
12. Sponsoring Agency Name and Address	13. Type of Report and Period Covered
National Aeronautics and Space Administration Washington, DC 20546	Contractor Report
	14. Sponsoring Agency Code 505-60-31

15. Supplementary Notes

Langley Technical Monitor: John C. Lin
SBIR Phase I Final Report

16. Abstract

An active flow control device to generate large-scale, periodic structures in a turbulent shear flow is developed. Together with adaptive optics, the device may be used on airborne laser platforms to reduce or eliminate optical distortion caused by the turbulence in the aircraft's boundary layer. A cyclic jet issuing from a spanwise slot is used to collect the turbulent boundary layer for a finite time and then release all of the flow instantaneously in one large eddy that convects downstream. Flow visualization and hot-film probe measurements are used together with pattern recognition algorithms to demonstrate the viability of the flow control method. A flat plate towed in a water channel is used as a test bed. The instantaneous velocity signal is used to compute important statistical quantities of the random velocity field, such as the mean, the root-mean-square, the spectral distribution, and the probability density function. When optimized for a given boundary layer, it is shown that the cyclic jet will produce periodic structures that are similar to the random, naturally occurring ones. These structures seem to trigger the onset of bursting events near the wall of the plate. Thus, the present device generates periodic structures in both the outer and inner regions of a turbulent boundary layer.

17. Key Words (Suggested by Authors(s))	18. Distribution Statement
Flow Control; Airborne Laser Platform; Large Eddy Structures; Turbulence Control; Cyclic Jet; Random Eddies; Periodic Eddies.	Unclassified-Unlimited Subject Category 34

19. Security Classif.(of this report)	20. Security Classif.(of this page)	21. No. of Pages	22. Price
Unclassified	Unclassified	54	A04

For sale by the National Technical Information Service, Springfield, Virginia 22161